# Electronic supplementary information

## Unusual C–O bonds cleavage of aromatic ethers in ruthenium complexes bearing a 2-alkoxypyridyl fragment

Danfeng Deng,‡ Bowen Hu,‡ Min Yang, and Dafa Chen*

MIIT Key Laboratory of Critical Materials Technology for New Energy Conversion and Storage, School of Chemical Engineering & Technology, Harbin Institute of Technology, Harbin 150001, People's Republic of China.

‡ D. Deng and B. Hu contributed equally to this work.

Table of Contents

## Screening Reactions of Catalysis

To find the optimal conditions for *β*-alkylation of secondary alcohols with primary alcohols, the coupling of 1-phenylethanol and benzyl alcohol was selected as a model reaction to test the catalytic activity of complexes **1-6** (Table S1). At 110 °C, in the presence of 0.5 equiv of *t*-BuOK, 0.5 mol% of complexes **1-6** and 2 mL toluene, the reactions proceeded well under nitrogen condition. It can be seen that complexes **1-3** showed comparable high catalytic activity with good selectivity. And the different yields and selectivities of **4** and **5** might be due to the decomposition during the transformation of **4** to **5** under basic condition. Complex **1** was then selected as the catalyst for further investigation because it was easiest to be prepared.

**Table S1. *β*-Alkylation of 1-phenylethanol with benzyl alcohol using Ru complexes 1-6**[a]

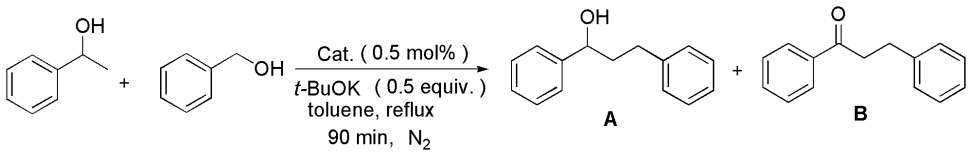


| entry | catalyst | conv[b] | A/B ratio[b] |
|---|---|---|---|
| 1 | **1** | 90 | 98:2 |
| 2 | **2** | 94 | 95:5 |
| 3 | **3** | 92 | 94:6 |
| 4 | **4** | 78 | 93:7[c] |
| 5 | **5** | 89 | 86:14 |
| 6 | **6** | 89 | 89:11 |

[a]Reaction condition: catalyst (0.5 mol%), 1-phenylethanol (1.0 mmol), benzyl alcohol (1.0 mmol) and *t*-BuOK (0.5 mmol) in reflux condition in toluene for 90 min under $N_2$ atmosphere. [b]Determined by GC analysis based on secondary alcohol. [c]The different yield and selectivity from those of **5** might be due to the decomposition during the transformation of **4** to **5**.

Subsequently, to optimize the reaction condition for *β*-alkylation of 1-phenylethanol with benzyl alcohol, different bases were explored. The weak bases such as $Na_2CO_3$, $K_2CO_3$ or $Cs_2CO_3$ revealed poor conversion, and *t*-BuOK was the most suitable one, indicating that a stronger base was beneficial to the desired product (Table S2, entries 1-6). If the reaction was carried out without a catalyst, the conversion was about 15% (Table S2, entry 7). Without a base, the reaction

could not take place (Table S2, entry 8).

**Table S2. *β*-Alkylation of 1-phenylethanol with benzyl alcohol in the presence of different bases**[a]

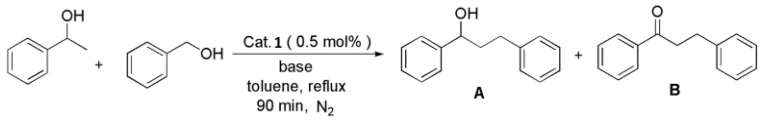


| entry | base (amt (equiv)) | conv (%)[b] |
|---|---|---|
| 1 | $Na_2CO_3$ (0.5 equiv.) | 5 |
| 2 | $K_2CO_3$ (0.5 equiv.) | 4 |
| 3 | $Cs_2CO_3$ (0.5 equiv.) | 7 |
| 4 | KOH (0.5 equiv.) | 83 |
| 5 | NaOH (0.5 equiv.) | 86 |
| 6 | *t*-BuOK (0.5 equiv.) | 90 |
| 7[c] | *t*-BuOK (0.5 equiv.) | 15 |
| 8 | No base | 0 |

[a]Reaction condition: catalyst **1** (0.5 mol%), 1-phenylethanol (1.0 mmol), benzyl alcohol (1.0 mmol) and base in reflux condition in toluene for 90 min under $N_2$ atmosphere. [b]Determined by GC analysis based on secondary alcohol. [c]No catalyst.

**1,3-Diphenylpropan-1-ol**.[1] $^1$H NMR (400 MHz, $CDCl_3$, ppm): 7.34−7.17 (m, 10H), 4.66 (t, J = 7.2 Hz, 1H), 2.77−2.61 (m, 2H), 2.16−1.96 (m, 2H), 1.84 (s, 1H).

**3-(2-Chlorophenyl)-1-phenylpropan-1-ol**.[1] $^1$H NMR (400 MHz, $CDCl_3$, ppm): 7.39−7.11 (m, 9H), 4.74-4.71 (m, 1H), 2.94−2.74 (m, 2H), 2.14−2.00 (m, 2H), 1.90 (s, 1H).

**3-(3-Chlorophenyl)-1-phenylpropan-1-ol**.[1] $^1$H NMR (400 MHz, $CDCl_3$, ppm): 7.35−7.12 (m, 8H), 7.05−7.03 (m, 1H), 4.65-4.62 (m, 1H), 2.74−2.58 (m, 2H), 2.12−1.93 (m, 2H), 1.90 (s, 1H).

**3-(4-Bromophenyl)-1-phenylpropan-1-ol**.[1] $^1$H NMR (400 MHz, $CDCl_3$, ppm): 7.39−7.24 (m, 7H), 7.04 (d, J = 8 Hz, 2H), 4.64 (dd, J = 7.6, 5.2 Hz, 1H), 2.72−2.57 (m, 2H), 2.13−1.92 (m, 3H).

**3-(4-Fluorophenyl)-1-phenylpropan-1-ol**.[1] $^1$H NMR (400 MHz, $CDCl_3$, ppm): 7.39−7.27 (m, 5H), 7.16−7.12 (m, 2H), 6.99−6.94 (m, 2H), 4.69-4.65 (m, 1H), 2.77−2.61 (m, 2H), 2.16− 1.97 (m, 2H), 1.93 (s, 1H).

**3-(4-Methoxyphenyl)-1-phenylpropan-1-ol**.[1] $^1$H NMR (400 MHz, $CDCl_3$, ppm): 7.38−7.27 (m, 5H), 7.12 (d, J = 8.8 Hz, 2H), 6.83 (d, J = 8.4 Hz, 2H), 4.70-4.66 (m, 1H), 3.79 (s, 3H), 2.74−2.58

(m, 2H), 2.16−1.96 (m, 2H), 1.87 (s, 1H).

**3-(3,4-Dimethoxyphenyl)-1-phenylpropan-1-ol**.[2] $^1$H NMR (400 MHz, $CDCl_3$, ppm): 7.36−7.27 (m, 5H), 6.80−6.72 (m, 3H), 4.70-4.67 (m, 1H), 3.86 (s, 6H), 2.75−2.59 (m, 2H), 2.17−1.97 (m, 2H), 1.91 (s, 1H).

**3-(Naphthalen-2-yl)-1-phenylpropan-1-ol**.[3] $^1$H NMR (400 MHz, $CDCl_3$, ppm): 7.83−7.78 (m, 3H), 7.65 (s, 1H), 7.49−7.30 (m, 8H), 4.75-4.72 (m, 1H), 2.97−2.84 (m, 2H), 2.29−2.09 (m, 2H), 1.92 (s, 1H).

**1-(4-Chlorophenyl)-3-phenylpropan-1-ol**.[1] $^1$H NMR (400 MHz, $CDCl_3$, ppm): 7.34−7.26 (m, 6H), 7.22−7.18 (m, 3H), 4.69-4.66 (m, 1H), 2.77−2.63 (m, 2H), 2.15−1.95 (m, 2H), 1.87 (s, 1H).q

**1-(4-Methoxyphenyl)-3-phenylpropan-1-ol**.[1] $^1$H NMR (400 MHz, $CDCl_3$, ppm): 7.30−7.17 (m, 7H), 6.89−6.87 (m, 2H), 4.63-4.60 (m, 1H), 3.80 (s, 3H), 2.76−2.59 (m, 2H), 2.17−1.95 (m, 3H).

**References**

1 B. C. Roy, K. Chakrabarti, S. Shee, S. Paul, S. Kundu, *Chem. - Eur. J.* 2016, **22**, 18147−18155.

2 J. Yang, X. Liu, D.-L. Meng, H.-Y. Chen, Z.-H. Zong, T.-T. Feng, K. Sun, *Adv. Synth. Catal.* 2012, **354**, 328−334.

3 H. W. Cheung, T. Y. Lee, H. Y. Lui, C. H. Yeung, C. P. Lau, *Adv. Synth. Catal.* 2008, **350**, 2975−2983.

## Crystallographic Details

**1:** A total of 24051 reflections (-15 ≤ *h* ≤ 16, -19 ≤ *k* ≤ 18, -20 ≤ *l* ≤ 20) were collected at *T* = 173.00(10) K in the range of 3.017 to 29.154° of which 11974 were unique ($R_{int}$ = 0.0401); $Mo_K$ radiation (λ = 0.71073 Å). The structure was solved by the direct methods. All non-hydrogen atoms were refined anisotropically, and hydrogen atoms were placed in calculated idealized positions. The residual peak and hole electron densities were 1.903 and -1.540 $eA^{-3}$, respectively. The least squares refinement converged normally with residuals of *R*(*F*) = 0.0975, *wR*($F^2$) = 0.2270 and a GOF = 1.056 ($I>2\sigma(I)$). $C_{52}H_{45}Cl_7N_2O_3P_2Ru$, Mw = 1157.06, space group P-1, Triclinic, *a* = 11.8566(5), *b* = 14.8810(5), *c* = 15.3961(5) Å, $\alpha$ = 83.417(3)°, $\beta$ = 87.037(3)°, $\gamma$ = 74.939(3)°, *V* = 2605.17(16) $Å^3$, *Z* = 2, $\rho_{calcd}$ = 1.475 $Mg/m^3$. CCDC-1860766 contains the supplementary crystallographic data for this paper. These data can be obtained free of charge from The Cambridge Crystallographic Data Centre via www.ccdc.cam.ac.uk/data_request/cif.

**2:** A total of 70016 reflections (-15 ≤ *h* ≤ 15, -24 ≤ *k* ≤ 25, -28 ≤ *l* ≤ 28) were collected at *T* = 173.00(2) K in the range of 2.033 to 28.276° of which 22855 were unique ($R_{int}$ = 0.0915); $Mo_K$ radiation (λ = 0.71073 Å). The structure was solved by the direct methods. All non-hydrogen atoms were refined anisotropically, and hydrogen atoms were placed in calculated idealized positions. The residual peak and hole electron densities were 3.108 and -1.400 $eA^{-3}$, respectively. The least squares refinement converged normally with residuals of *R*(*F*) = 0.0977, *wR*($F^2$) = 0.1919 and a GOF = 1.033 ($I>2\sigma(I)$). $C_{51}H_{47}ClN_2O_{5.50}P_2Ru_1$, Mw = 974.36, space group P-1, Triclinic, *a* = 11.7433(6), *b* = 19.4520(9), *c* = 21.6447(11) Å, $\beta$ = 79.871(2), *V* = 4625.3(4) $Å^3$, *Z* = 4, $\rho_{calcd}$ = 1.399 $Mg/m^3$. CCDC-1892620 contains the supplementary crystallographic data for this paper. These data can be obtained free of charge from The Cambridge Crystallographic Data Centre via www.ccdc.cam.ac.uk/data_request/cif.

**4a:** A total of 11861 reflections (-18 ≤ $h$ ≤ 17, -19 ≤ $k$ ≤ 19, -19 ≤ $l$ ≤ 16) were collected at $T$ = 173.00(10) K in the range of 2.618 to 28.317 of which 19784 were unique ($R_{int}$ = 0.0365); $Mo_K$ radiation (λ = 0.71073 Å). The structure was solved by the direct methods. All non-hydrogen atoms were refined anisotropically, and hydrogen atoms were placed in calculated idealized positions. The residual peak and hole electron densities were 0.684 and -0.789 $eA^{-3}$, respectively. The least squares refinement converged normally with residuals of $R(F)$ = 0.0624, $wR(F^2)$ = 0.1199 and a GOF = 1.027 ($I>2\sigma(I)$). $C_{51}H_{47}N_2O_2P_2Ru$, Mw = 11731.06, space group P1, Triclinic, $a$ = 13.5226(7), $b$ = 14.6020(7), $c$ = 14.9635(6) Å, $\alpha$ = 95.1960(10)°, $\beta$ = 115.0700(10)°, $\gamma$ = 104.090(2)°, $V$ = 2531.9(2) $Å^3$, $Z$ = 2, $\rho_{calcd}$ = 1.484 $Mg/m^3$. CCDC-1906744 contains the supplementary crystallographic data for this paper. These data can be obtained free of charge from The Cambridge Crystallographic Data Centre via www.ccdc.cam.ac.uk/data_request/cif.

**6:** A total of 11861 reflections (-14 ≤ $h$ ≤ 14, -19 ≤ $k$ ≤ 19, -24 ≤ $l$ ≤ 24) were collected at $T$ = 303.15 K in the range of 2.408 to 26.897 of which 13837 were unique ($R_{int}$ = 0.0993); $Mo_K$ radiation (λ = 0.71073 Å). The structure was solved by the direct methods. All non-hydrogen atoms were refined anisotropically, and hydrogen atoms were placed in calculated idealized positions. The residual peak and hole electron densities were 1.022 and -0.894 $eA^{-3}$, respectively. The least squares refinement converged normally with residuals of $R(F)$ = 0.1404, $wR(F^2)$ = 0.1951 and a GOF = 1.021 ($I>2\sigma(I)$).$C_{48}H_{41}Cl_3N_2O_2P_2Ru$, Mw = 947.19, space group P-1, Triclinic, $a$ = 10.2506(4), $b$ = 13.7227(5), $c$ = 17.3369(6) Å, $\alpha$ = 101.8130(10), $\beta$ = 106.7340(10), $\gamma$ = 94.5840(10) °, $V$ = 2260.75(14) $Å^3$, $Z$ = 2, $\rho_{calcd}$ = 1.391 $Mg/m^3$. CCDC-1942286 contains the supplementary crystallographic data for this paper. These data can be obtained free of charge from The Cambridge Crystallographic Data Centre via www.ccdc.cam.ac.uk/data_request/cif.

## IR Spectra

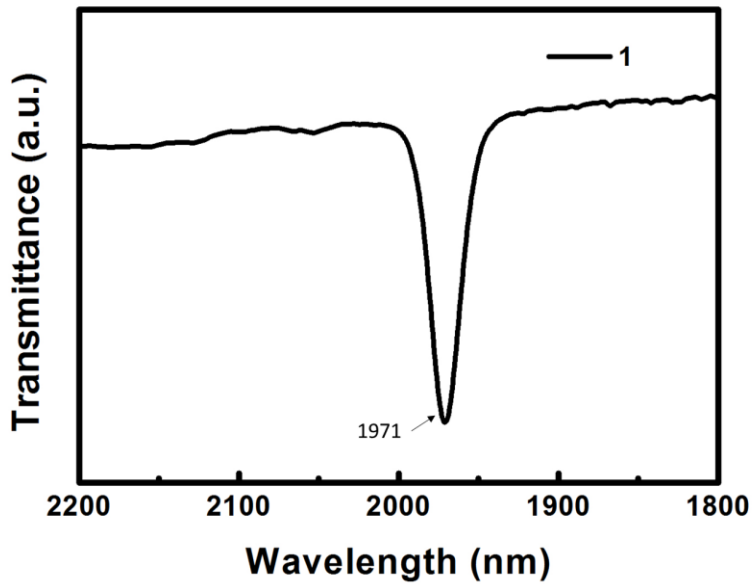


Fig. S1 IR spectrum of **1**.

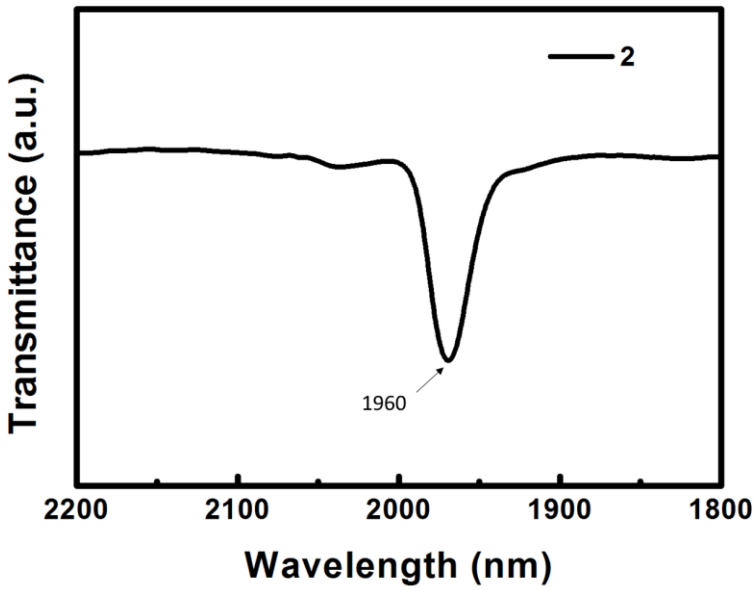


Fig. S2 IR spectrum of **2**.

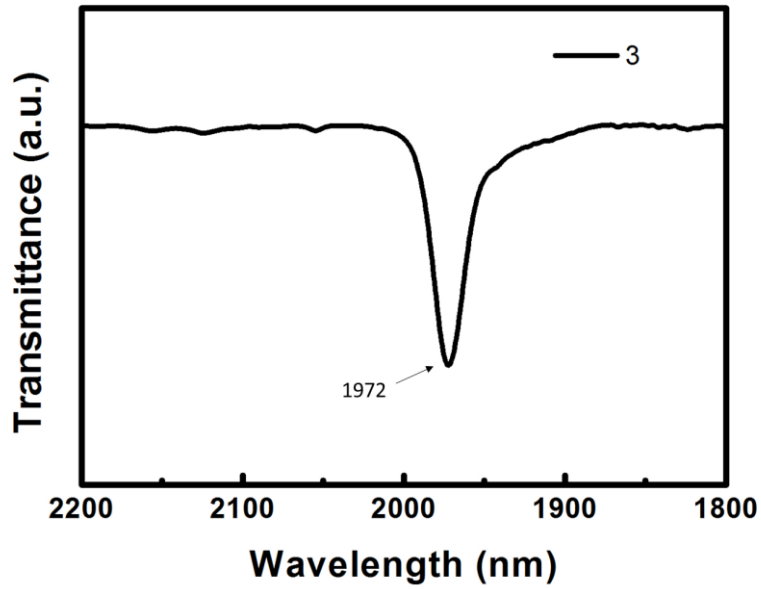


Fig. S3 IR spectrum of **3**.

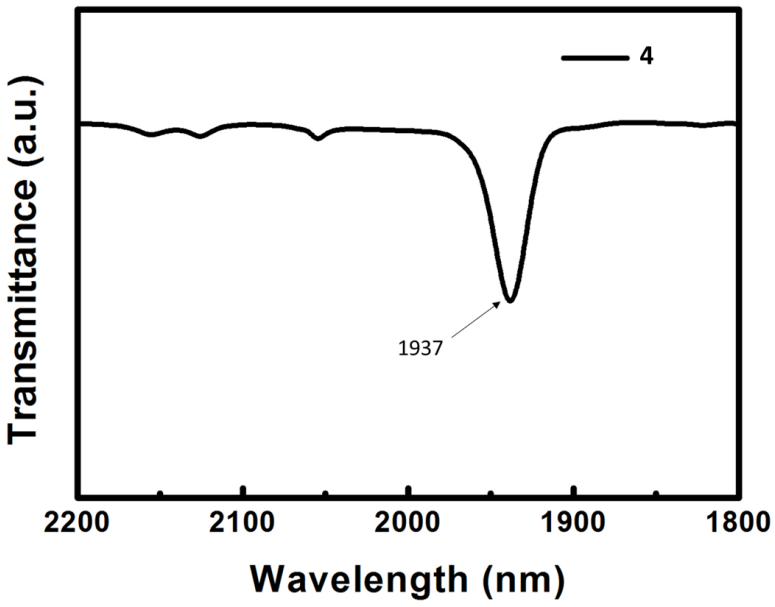


Fig. S4 IR spectrum of the mixture of **4a** and **4b**.

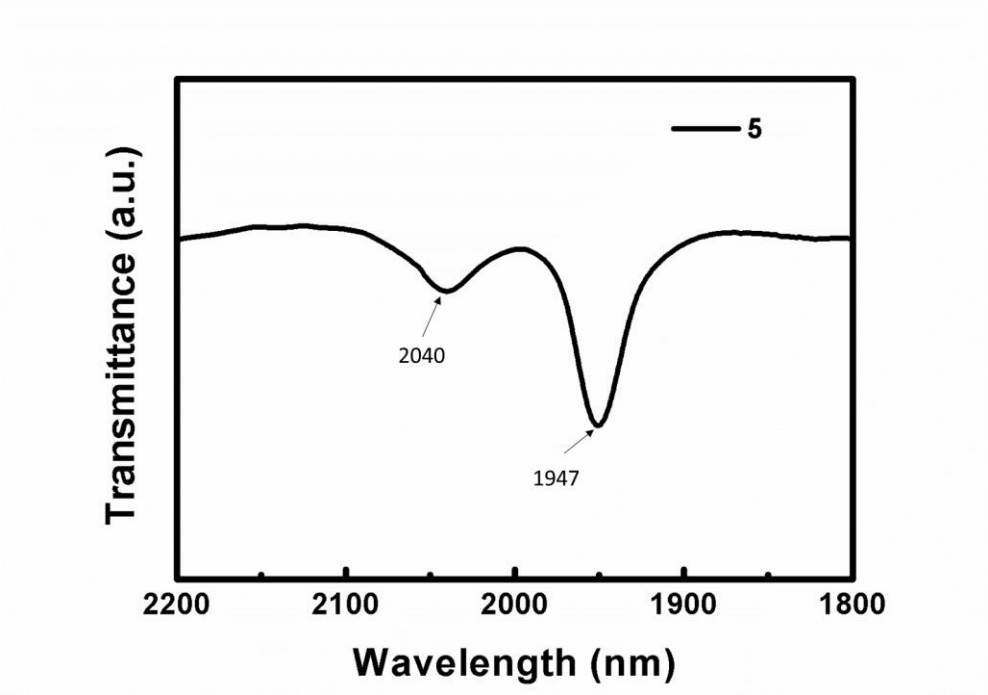


Fig. S5 IR spectrum of **5**.

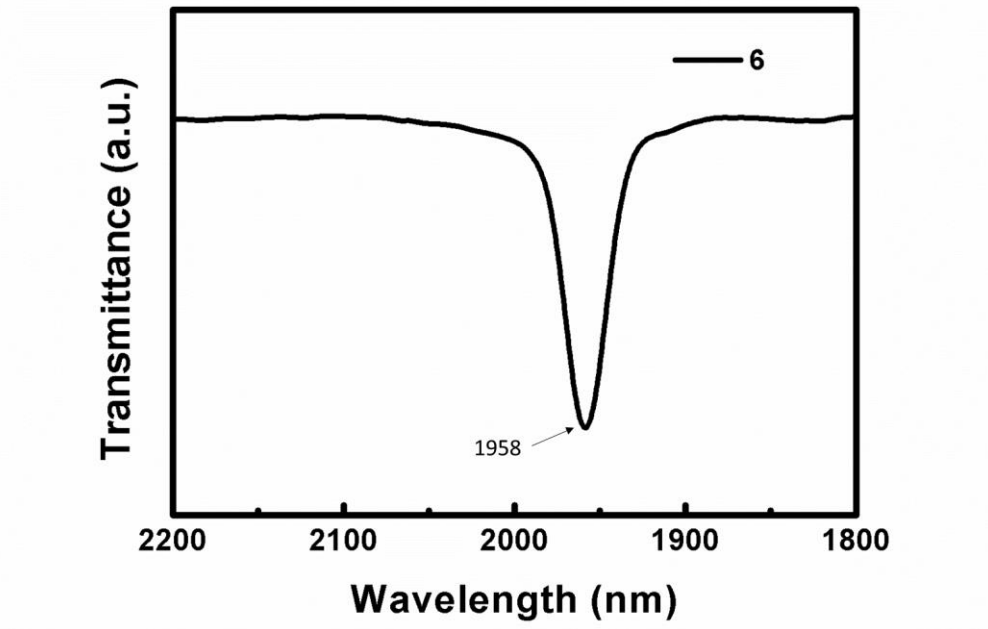


Fig. S6 IR spectrum of **6**.

# $^{1}$H NMR Spectra

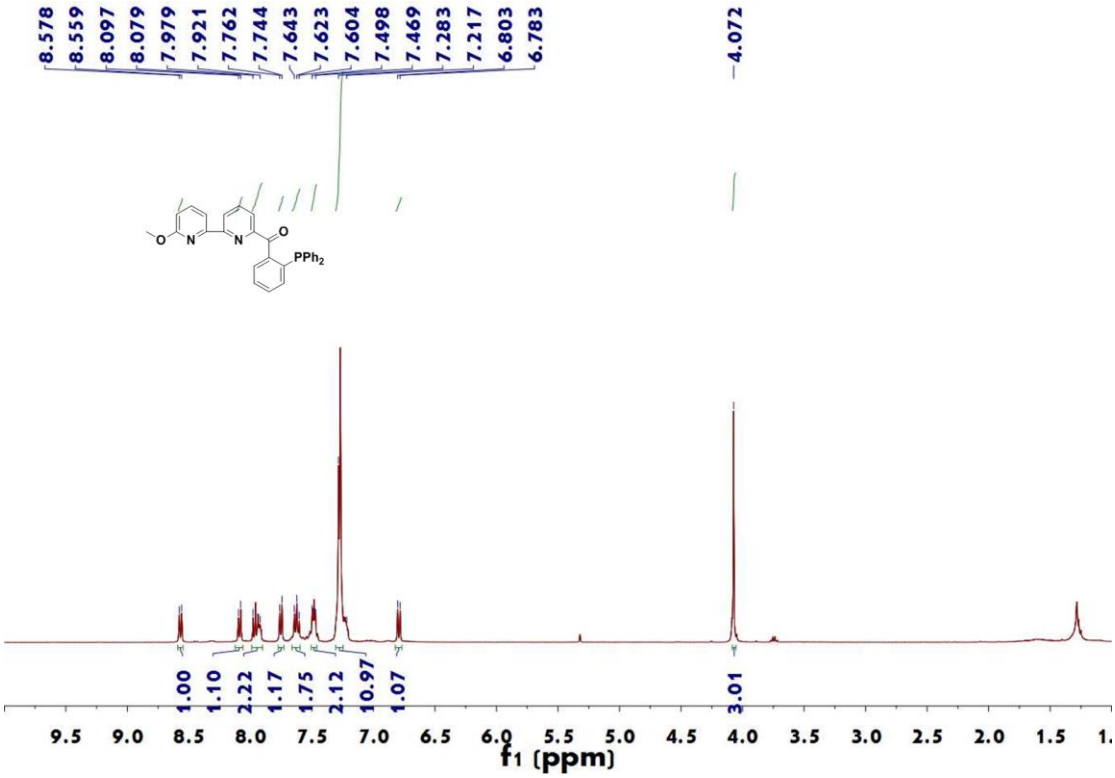


Fig. S7 $^{1}$H NMR spectrum of **L$_1$** in $CDCl_3$.

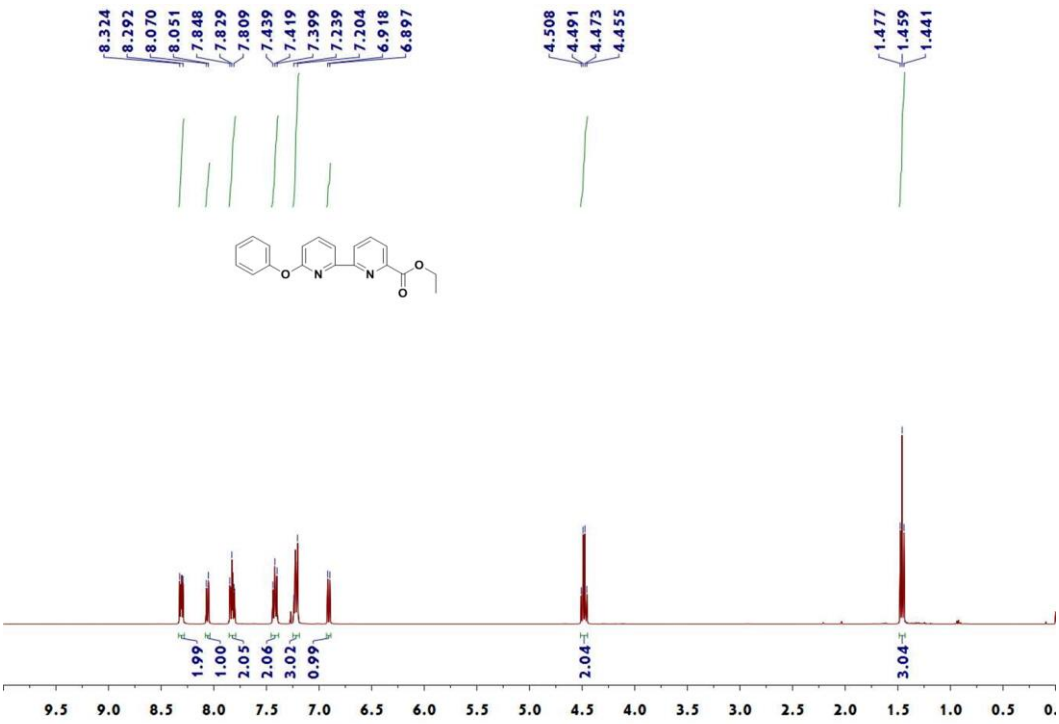


Fig. S8 $^{1}$H NMR spectrum of ethyl 6-(6-phenyloxypyridin-2-yl)pyridine-2-carboxylate in $CDCl_3$.

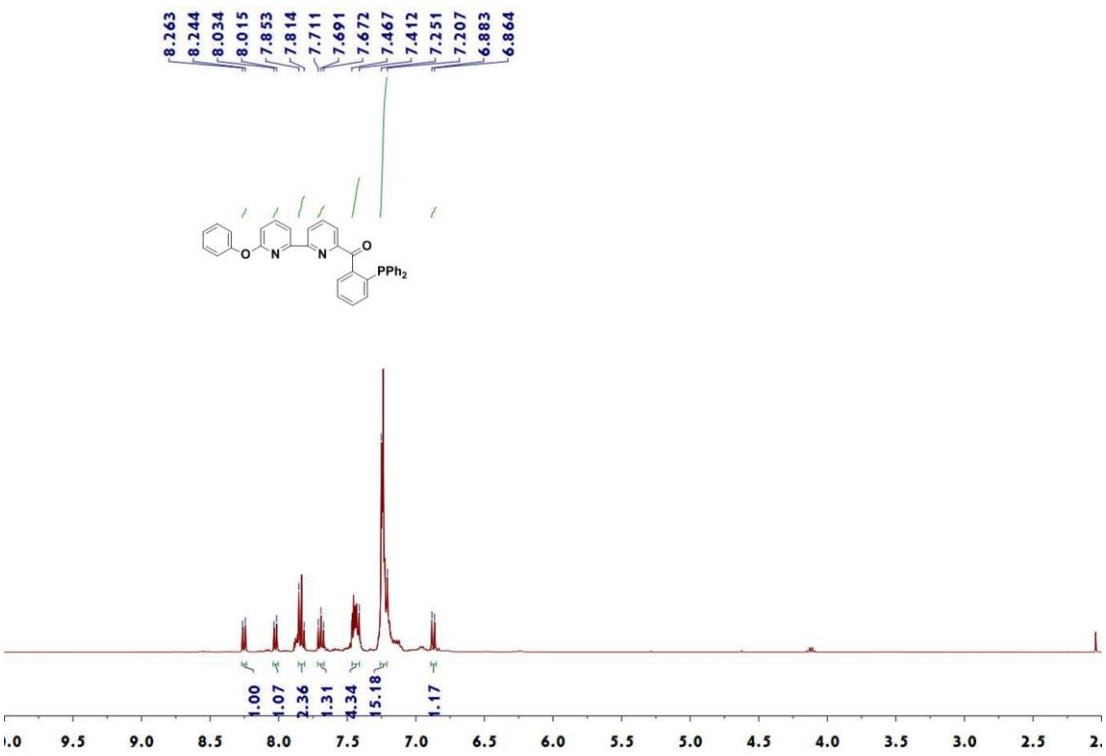


Fig. S9 $^{1}$H NMR spectrum of **L$_2$** in $CDCl_3$.

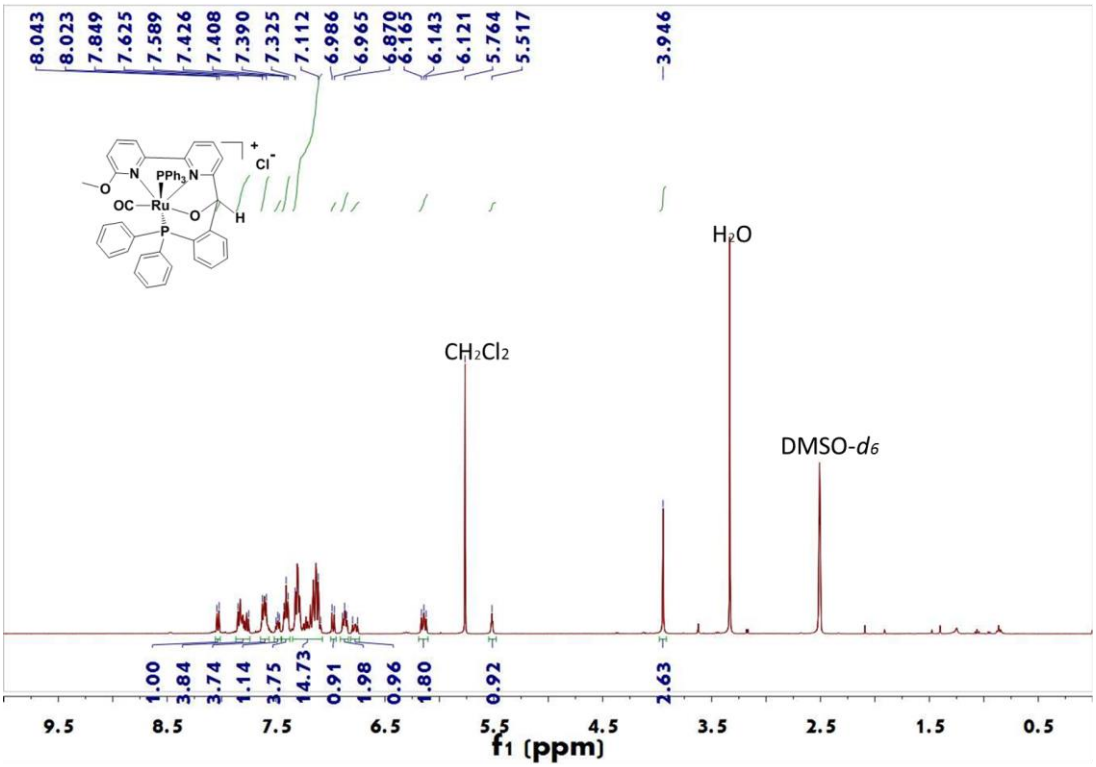


Fig. S10 $^{1}$H NMR spectrum of **1** in DMSO-$d_6$.

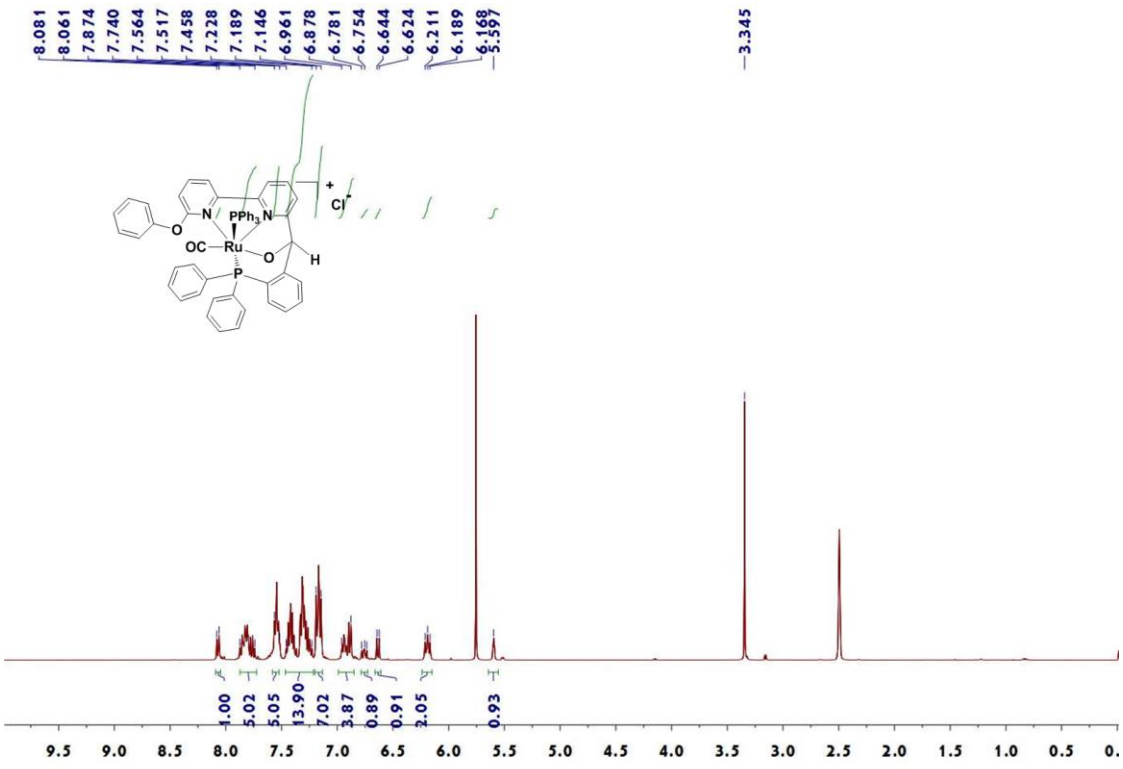


Fig. S11 $^{1}$H NMR spectrum of **3** in DMSO-$d_6$.

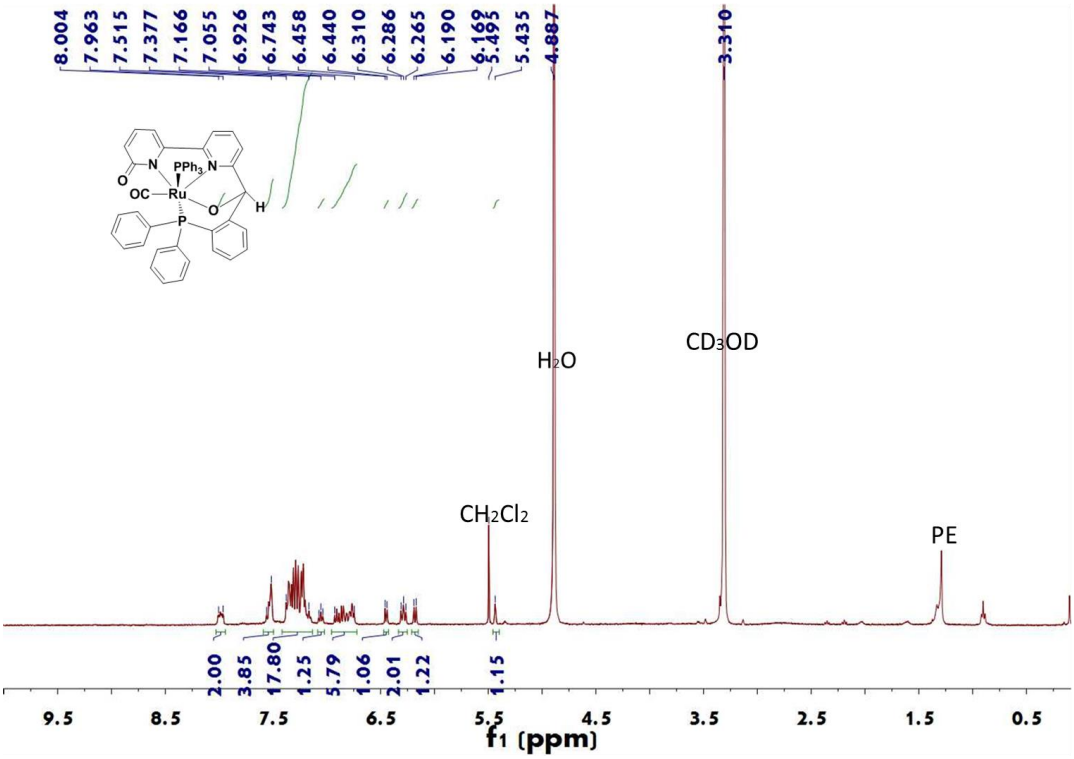


Fig. S12 $^{1}$H NMR spectrum of **2** in $CD_3OD$.

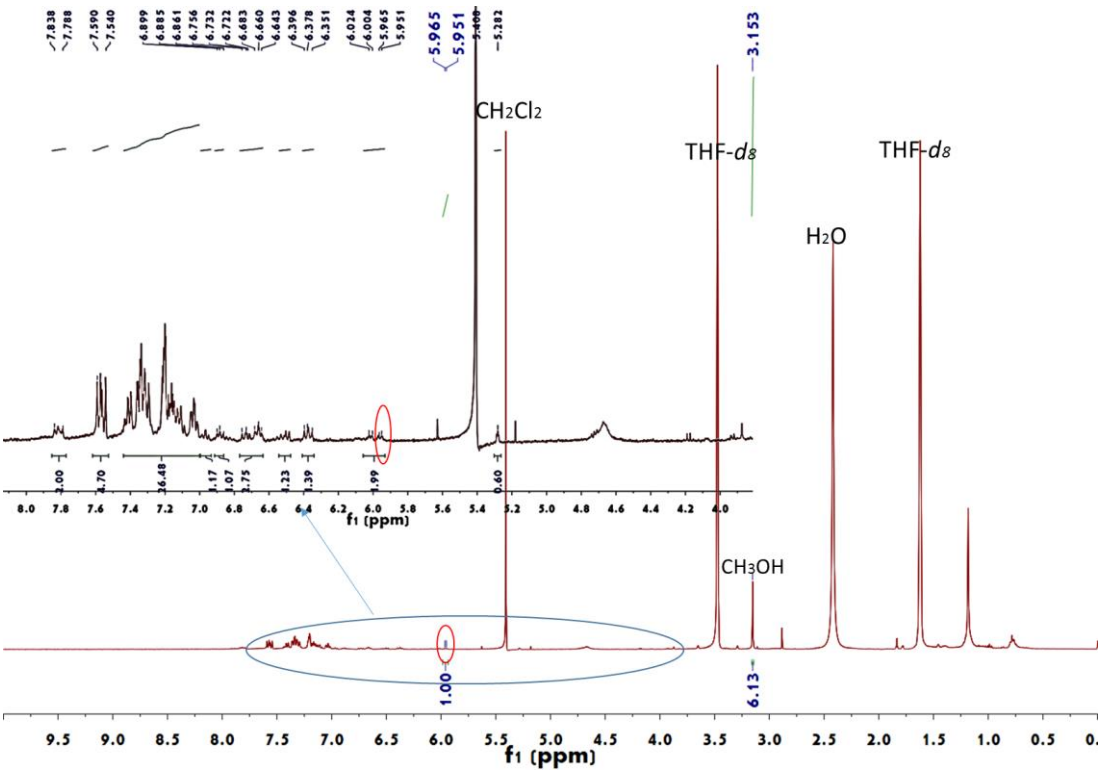


Fig. S13 $^{1}$H NMR spectrum of the reaction of complex **1** with $H_2O$ in THF-$d_8$ ($CH_3OH$ rather than $CH_3Cl$ was formed).

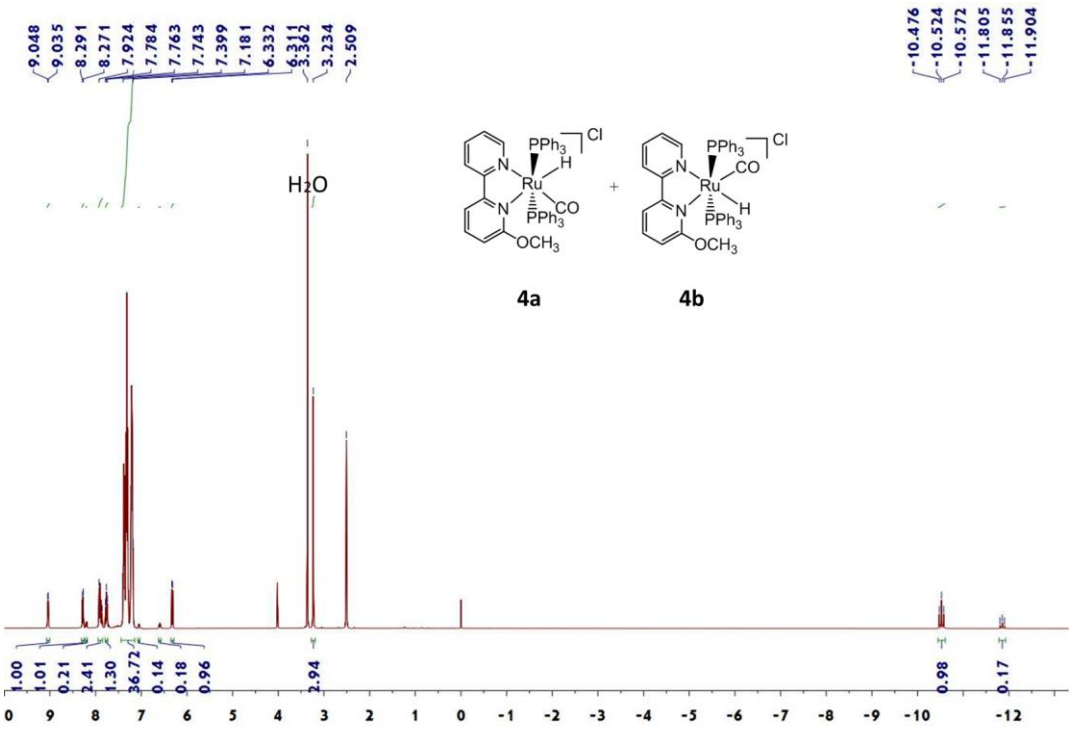


Fig. S14 $^{1}$H NMR spectrum of the mixture of **4a** and **4b** in DMSO-$d_6$.

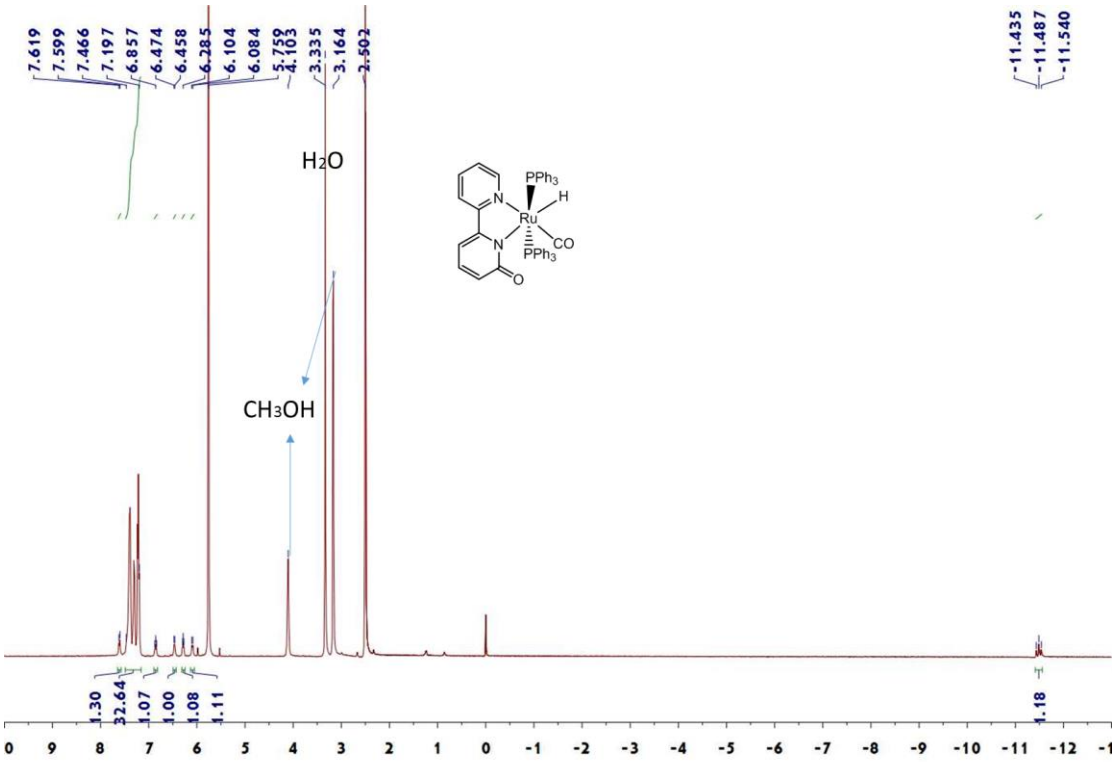


Fig. S15 $^{1}$H NMR spectrum of the mixture of **5** in DMSO-$d_6$.

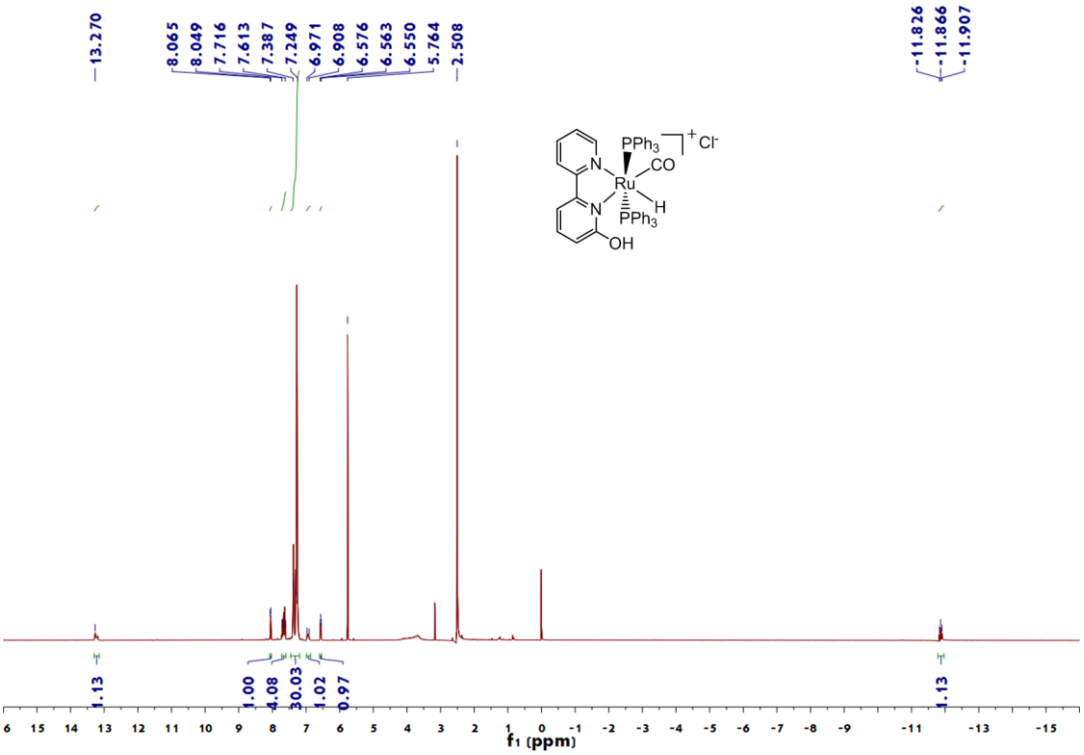


Fig. S16 $^{1}$H NMR spectrum of the mixture of **6** in DMSO-$d_6$.

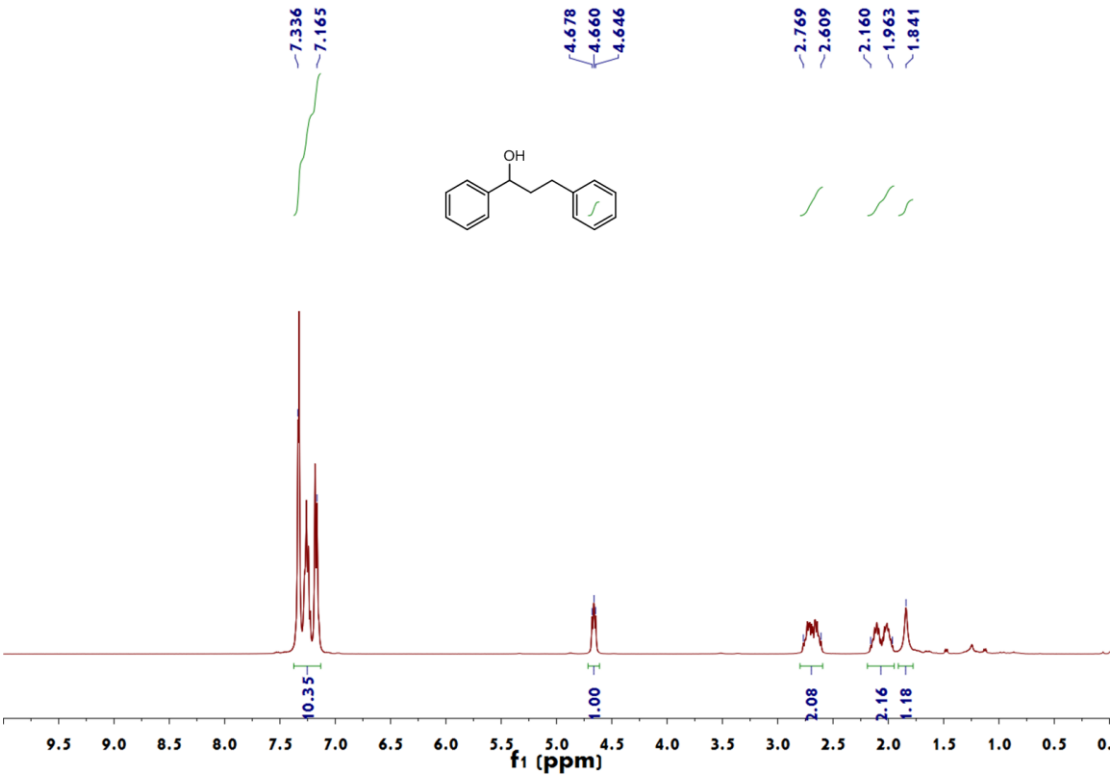


Figure S17. $^{1}H$ NMR spectrum of 1,3-diphenylpropan-1-ol in $CDCl_3$.

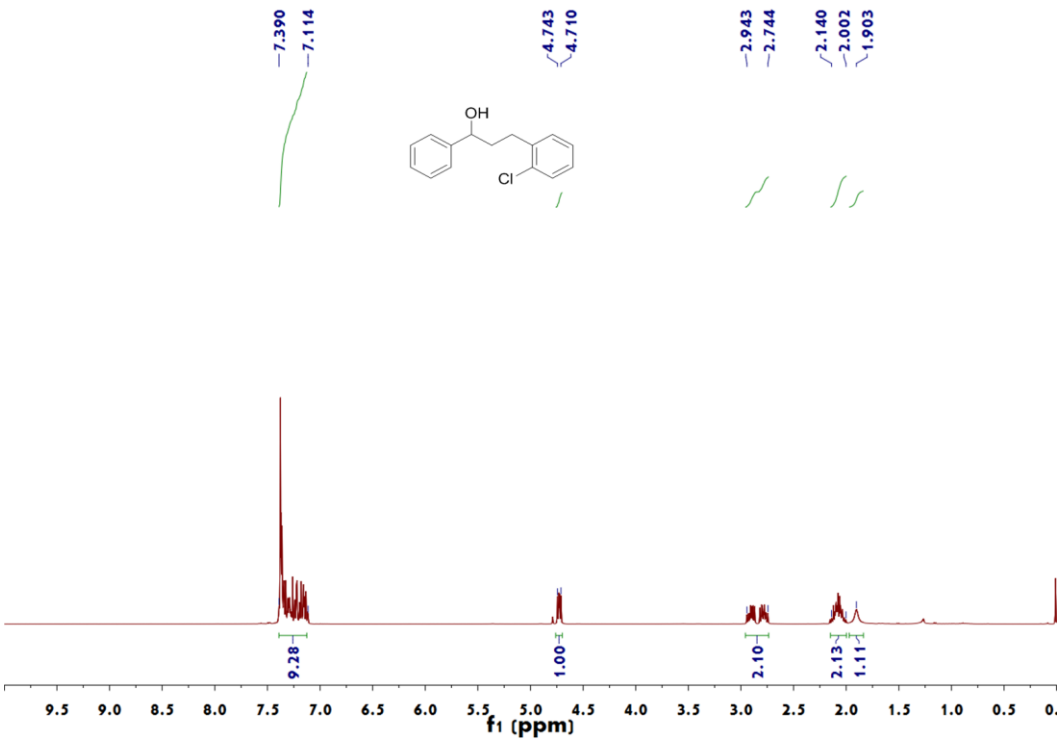


Figure S18. $^{1}H$ NMR spectrum of 3-(2-chlorophenyl)-1-phenylpropan-1-ol in $CDCl_3$.

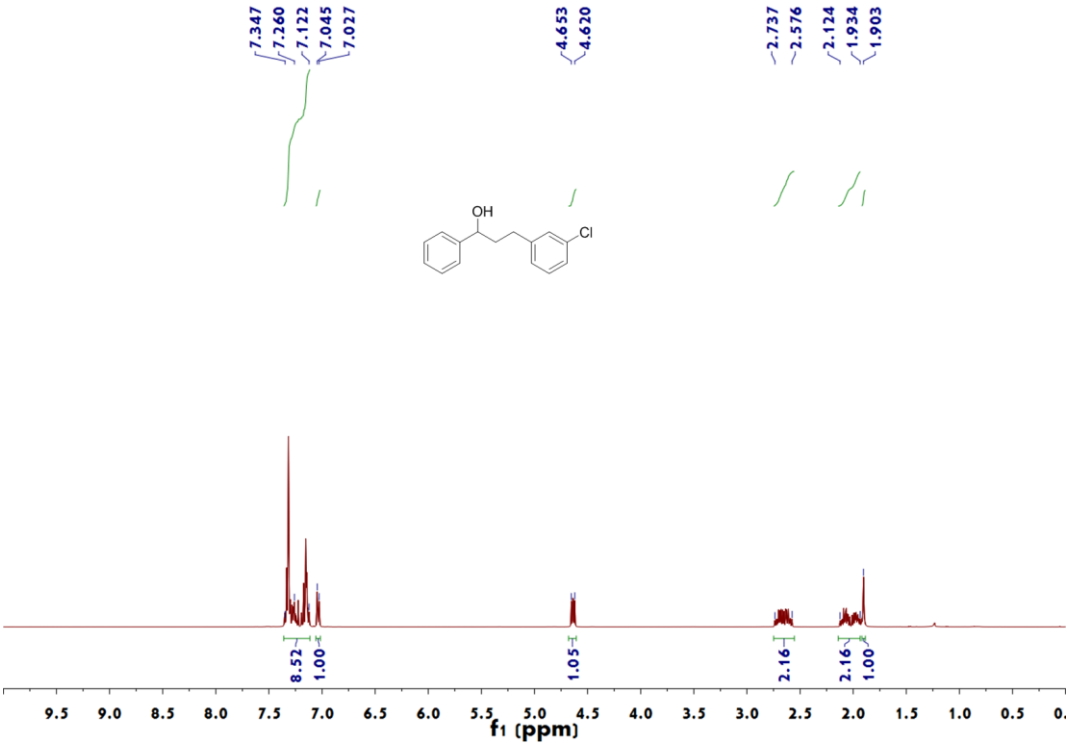


Figure S19. $^{1}$H NMR spectrum of 3-(3-chlorophenyl)-1-phenylpropan-1-ol in $CDCl_3$.

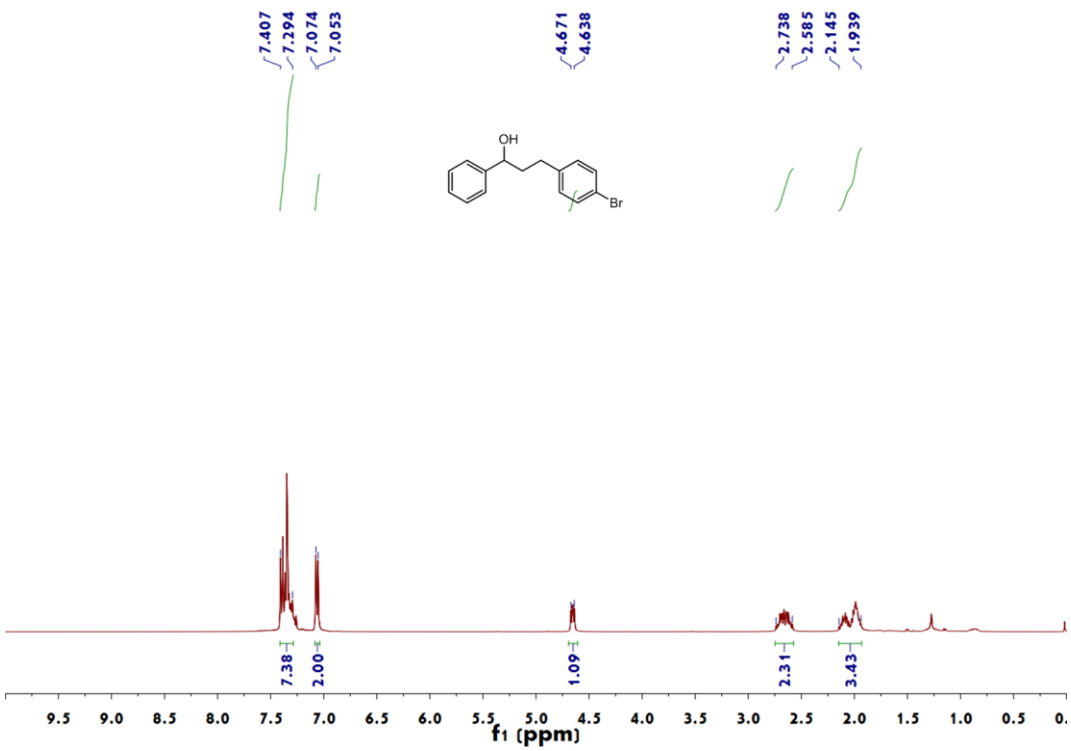


Figure S20. $^{1}$H NMR spectrum of 3-(4-bromophenyl)-1-phenylpropan-1-ol in $CDCl_3$.

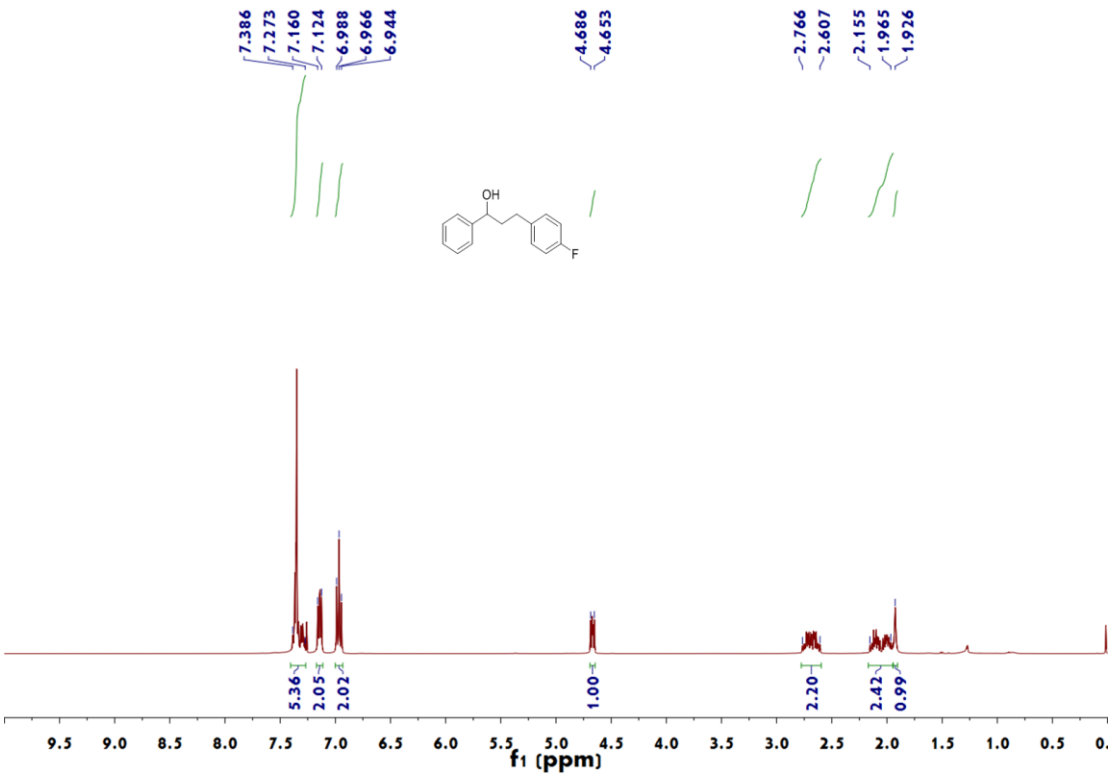


Figure S21. $^{1}H$ NMR spectrum of 3-(4-fluorophenyl)-1-phenylpropan-1-ol in $CDCl_3$.

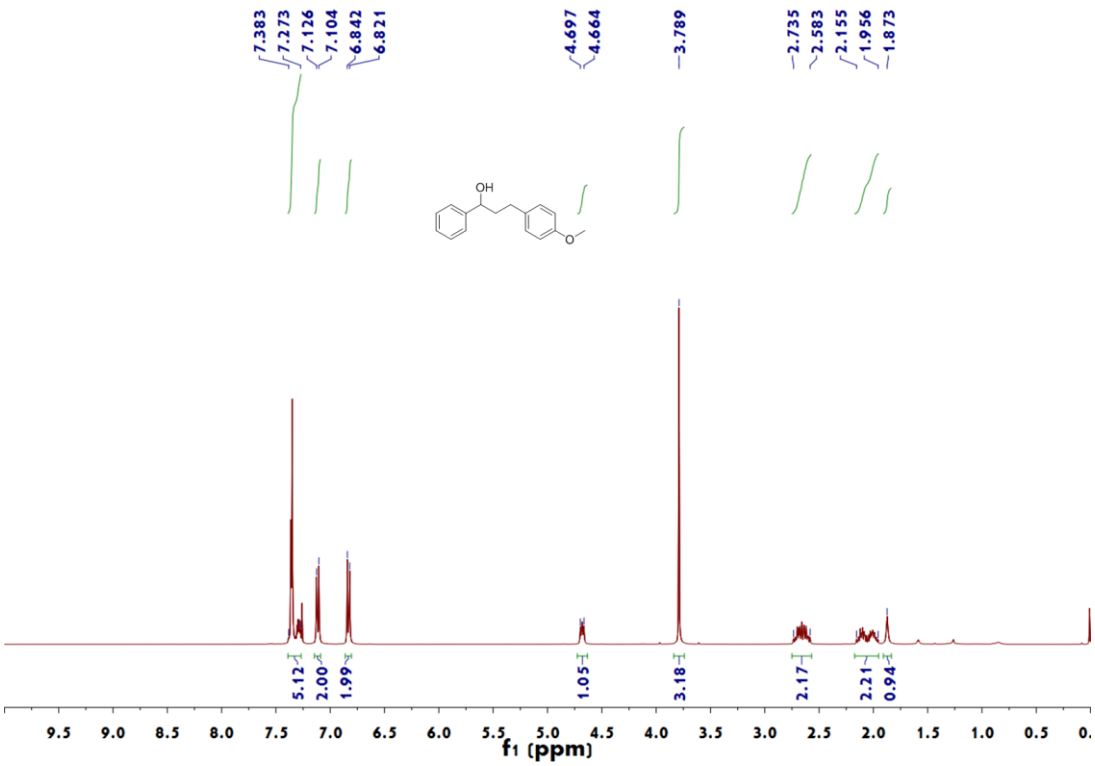


Figure S22. $^{1}H$ NMR spectrum of 3-(4-methoxyphenyl)-1-phenylpropan-1-ol in $CDCl_3$.

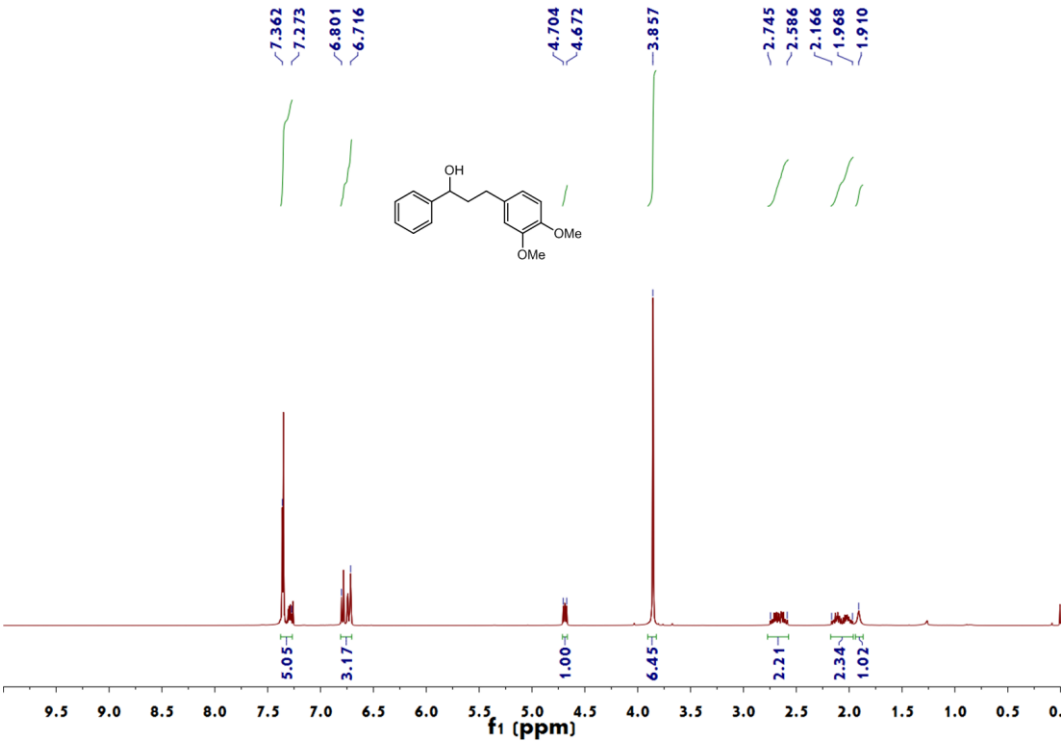


Figure S23. $^{1}$H NMR spectrum of 3-(3,4-dimethoxyphenyl)-1-phenylpropan-1-ol in $CDCl_3$.

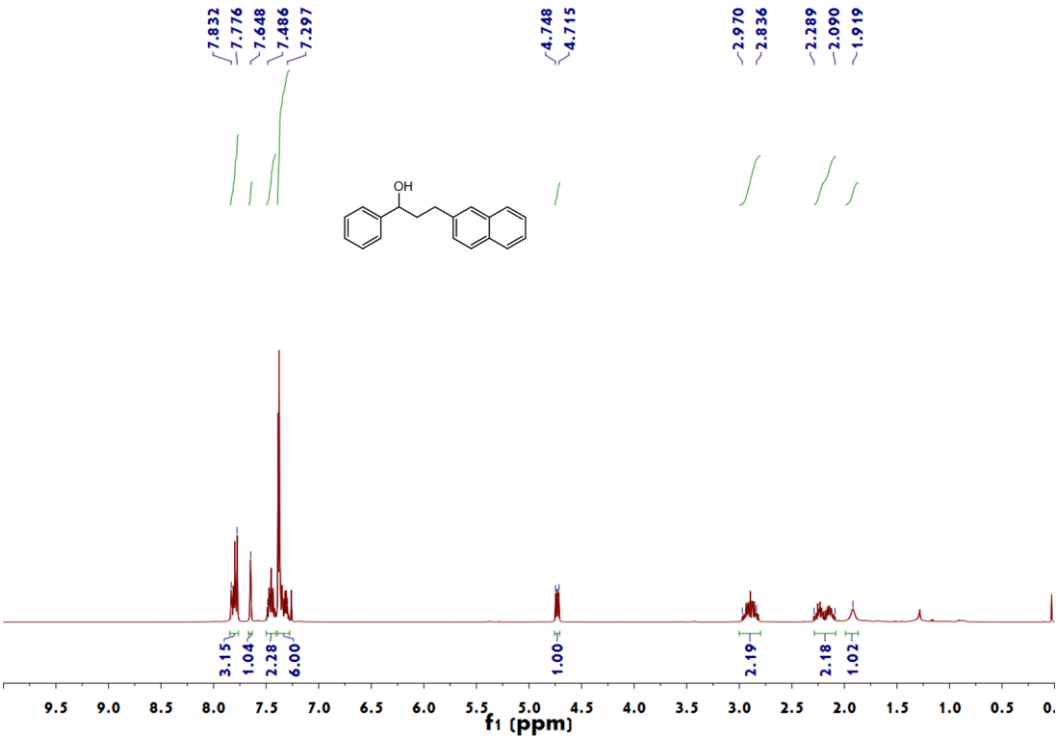


Figure S24. $^{1}H$ NMR spectrum of 3-(naphthalen-2-yl)-1-phenylpropan-1-ol in $CDCl_3$.

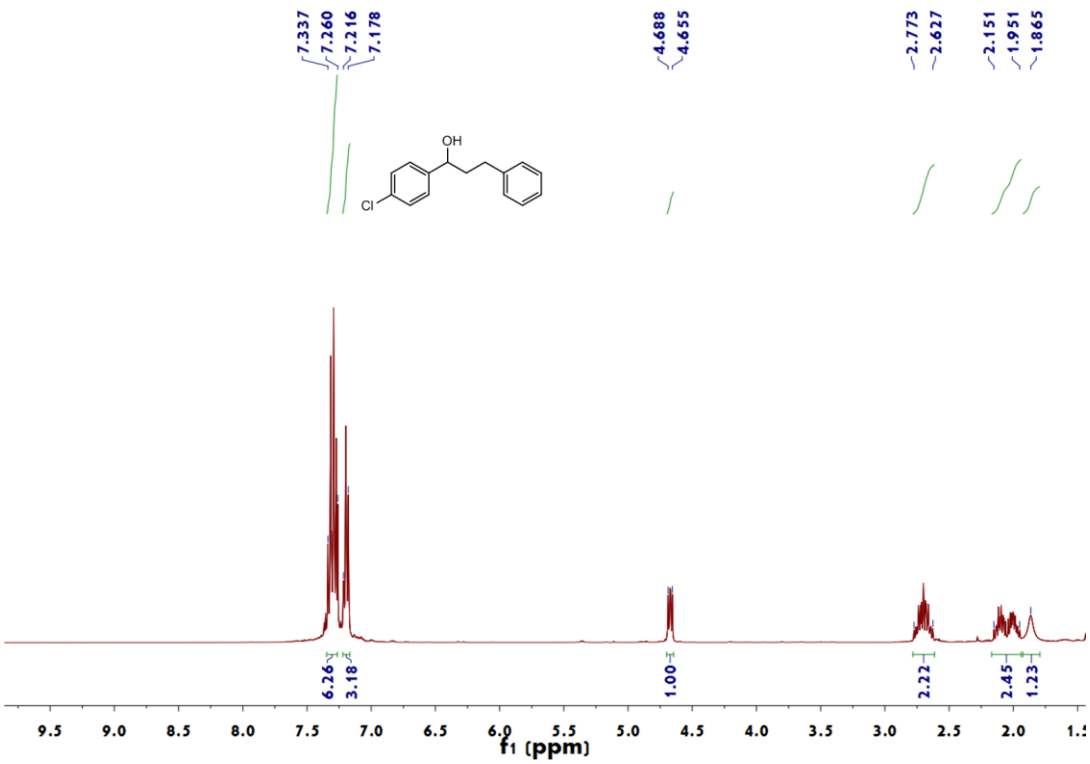


Figure S25. $^{1}H$ NMR spectrum of 1-(4-chlorophenyl)-3-phenylpropan-1-ol in $CDCl_3$.

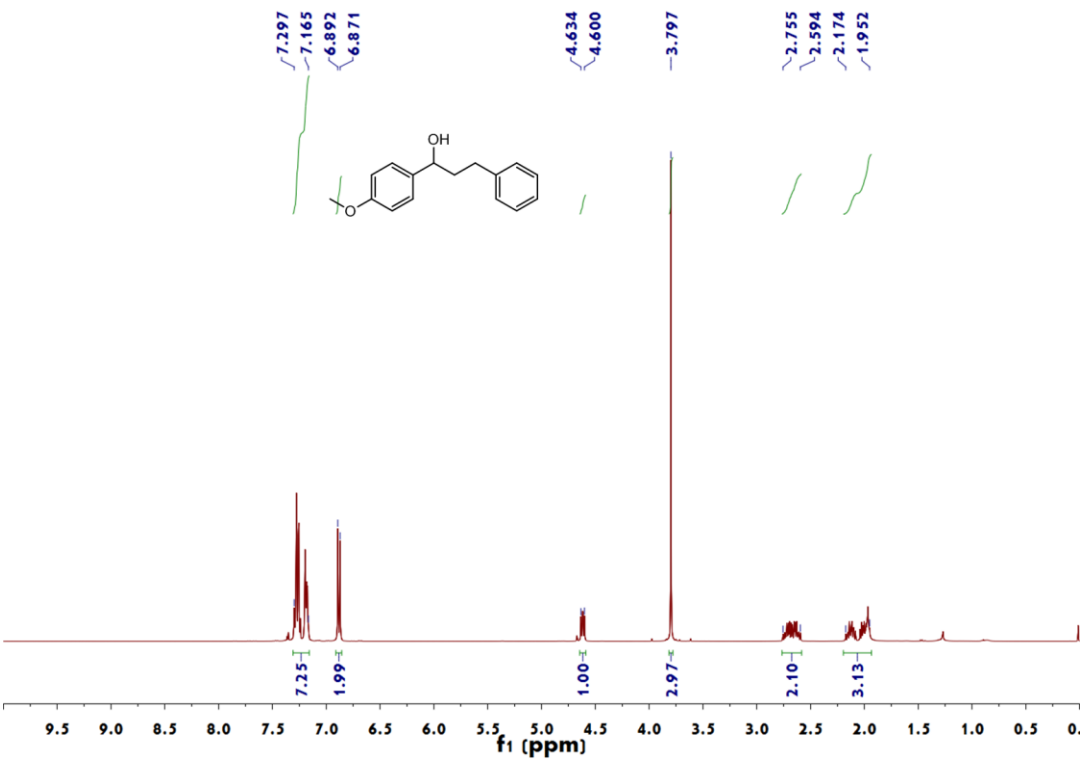


Figure S26. $^{1}H$ NMR spectrum of 1-(4-methoxyphenyl)-3-phenylpropan-1-ol in $CDCl_3$.

# $^{31}$P NMR Spectra

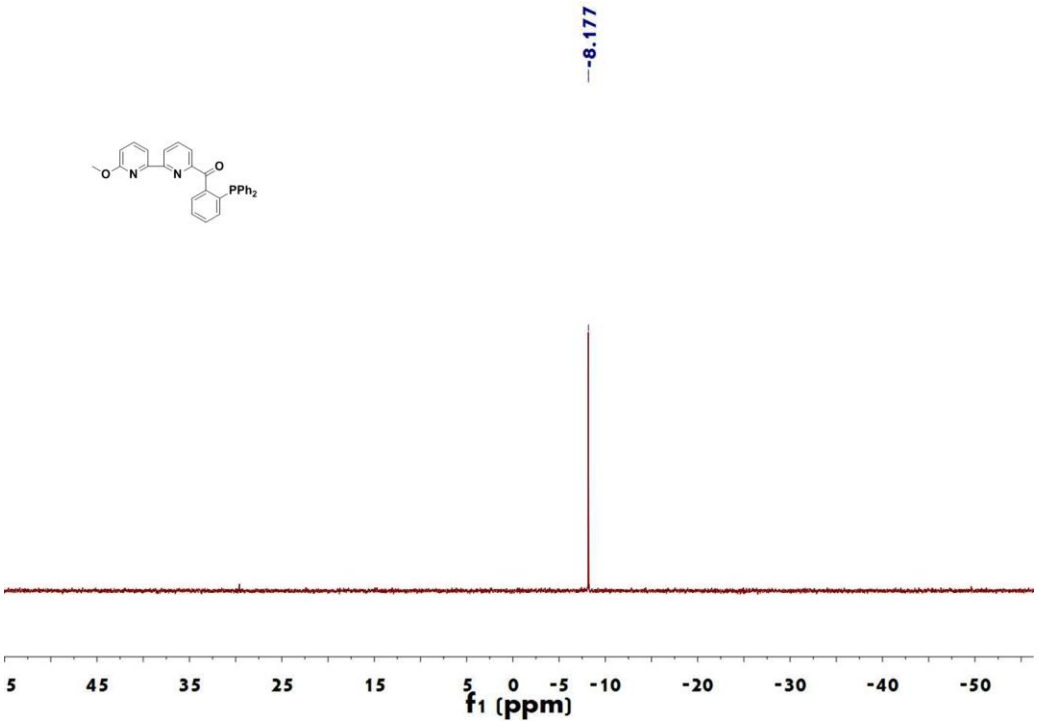


Fig. S27 $^{31}$P NMR spectrum of **L$_1$** in $CDCl_3$.

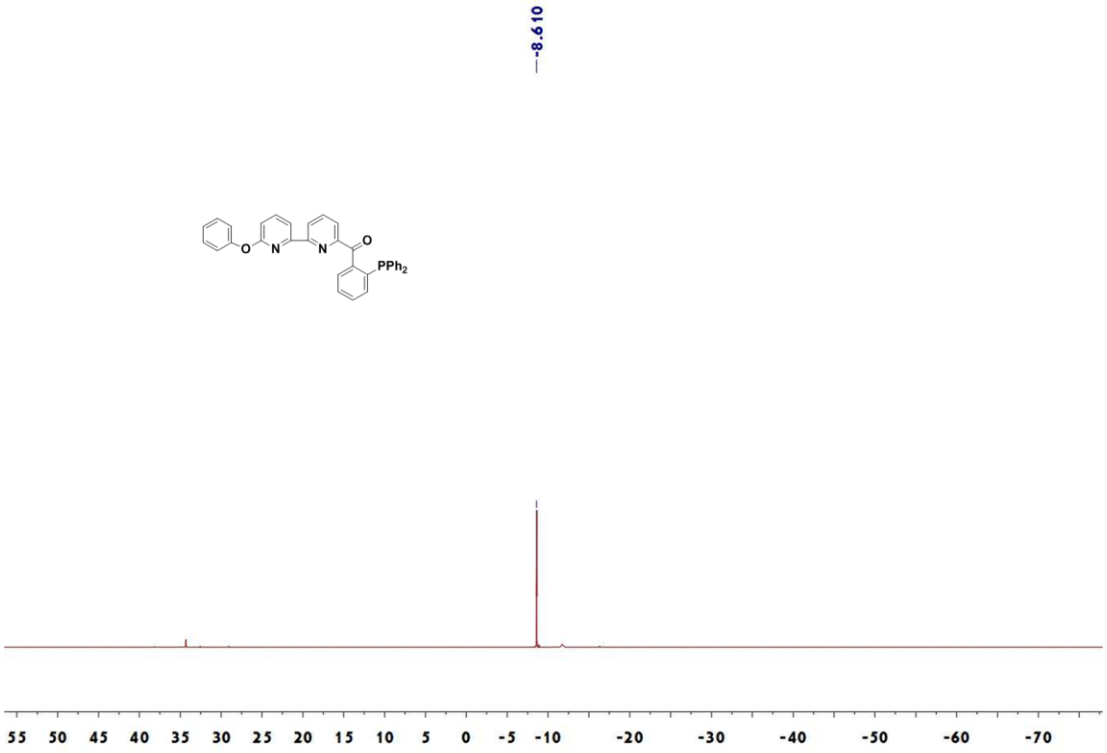


Fig. S28 $^{31}P$ NMR spectrum of $\mathbf{L_2}$ in $CDCl_3$.

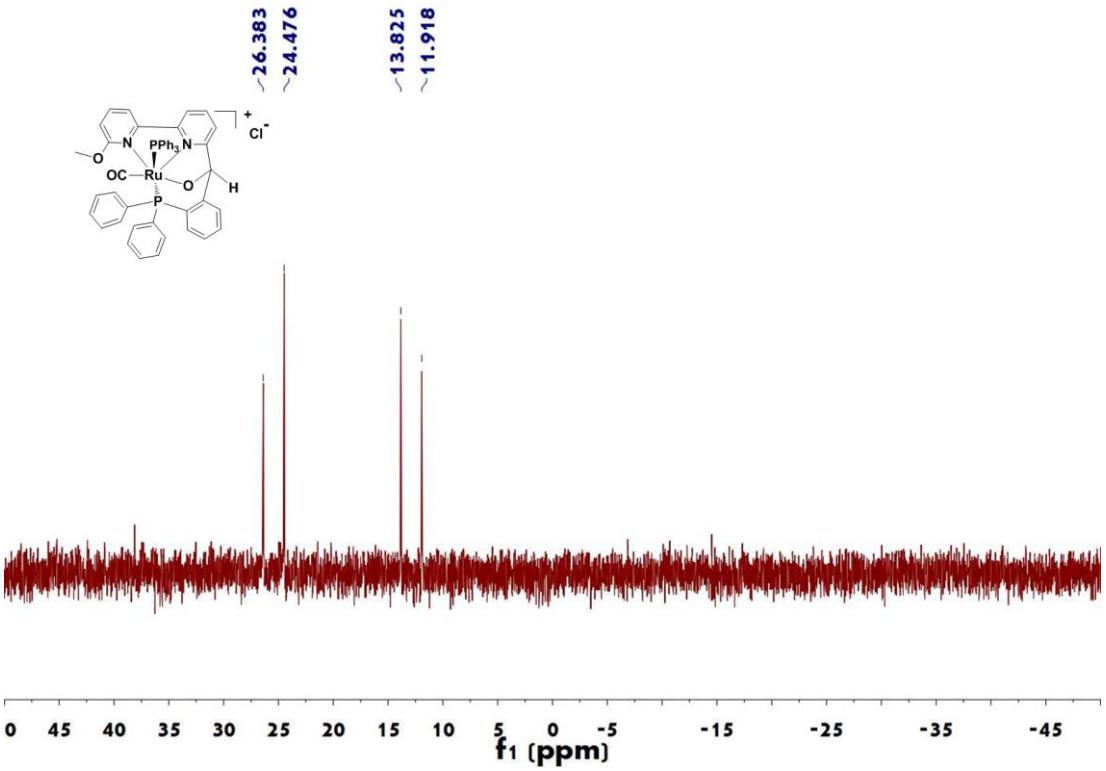


Fig. S29 $^{31}$P NMR spectrum of **1** in DMSO-*d*$_6$.

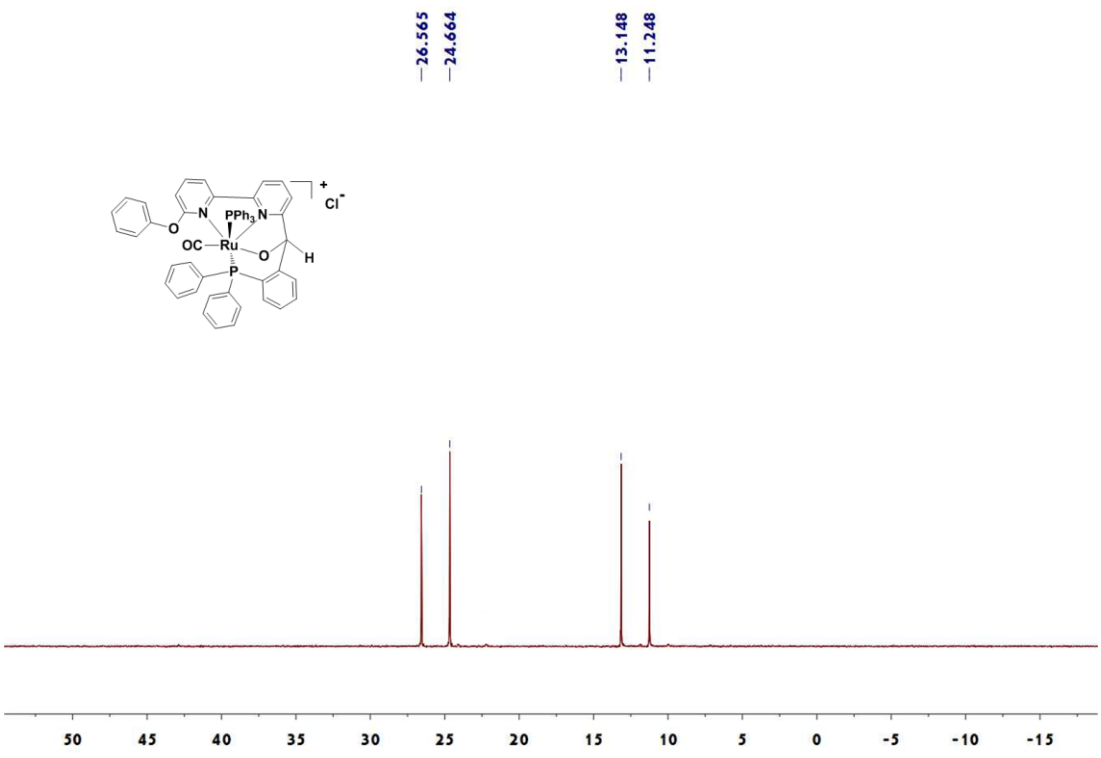


Fig. S30 $^{31}$P NMR spectrum of **3** in $CDCl_3$.

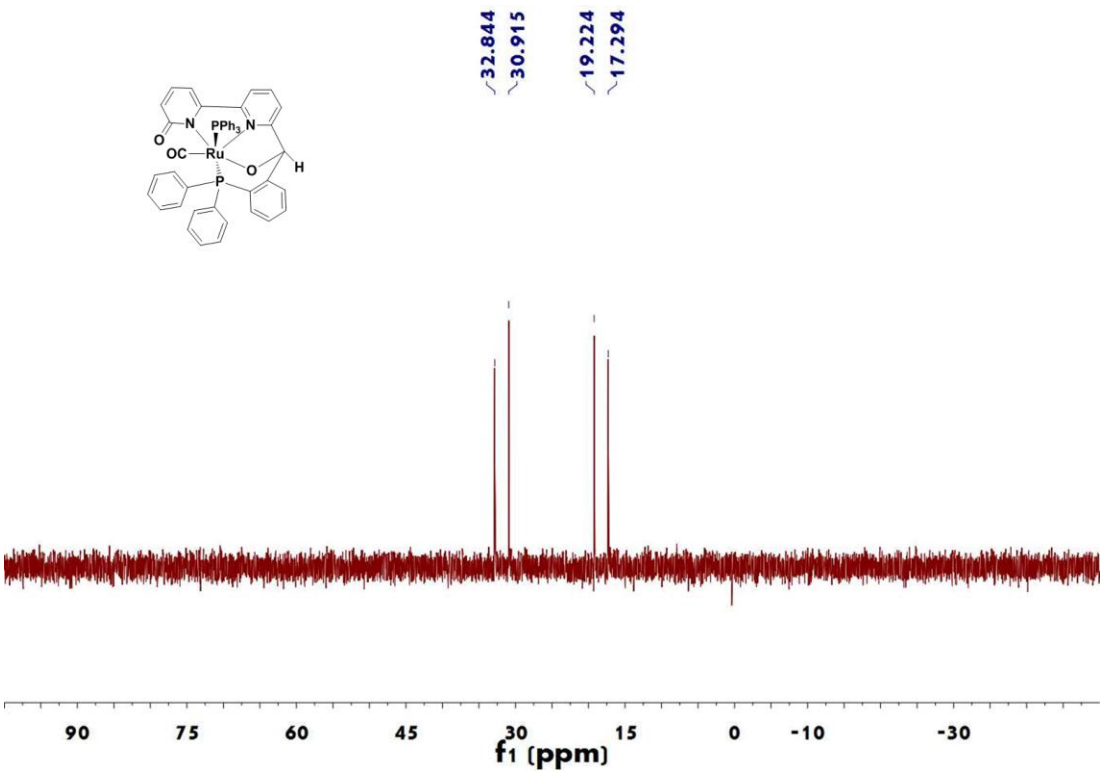


Fig. S31 $^{31}P$ NMR spectrum of **2** in $CD_3OD$.

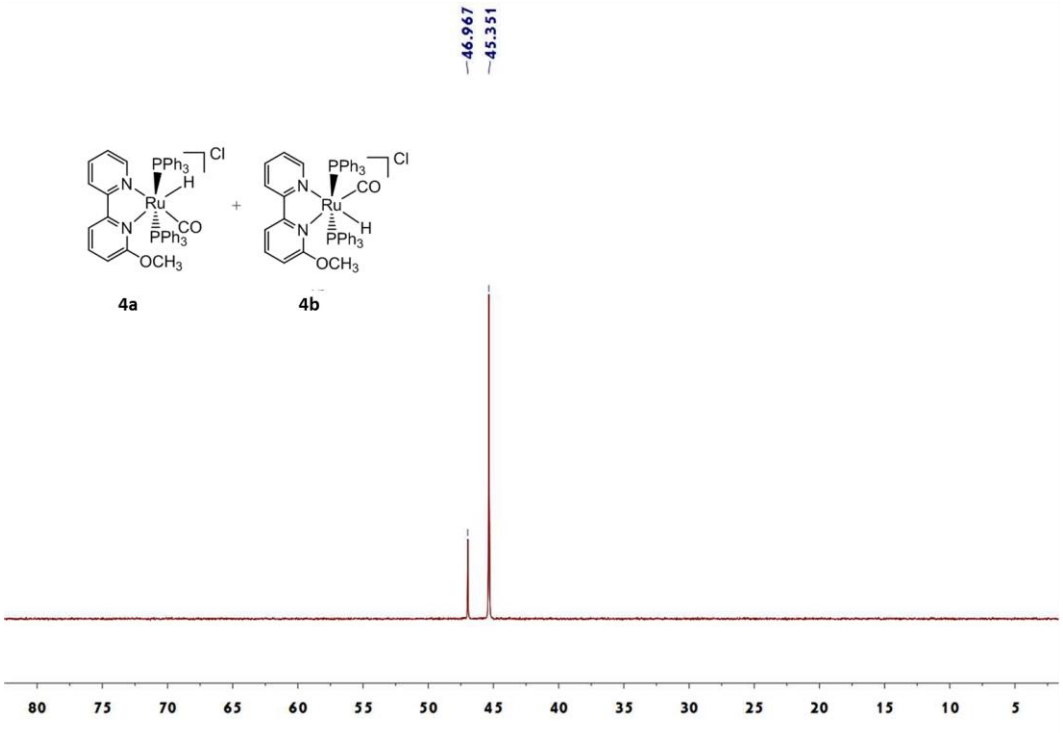


Fig. S32 $^{31}$P NMR spectrum of the mixture of **4a** and **4b** in DMSO-$d_6$.

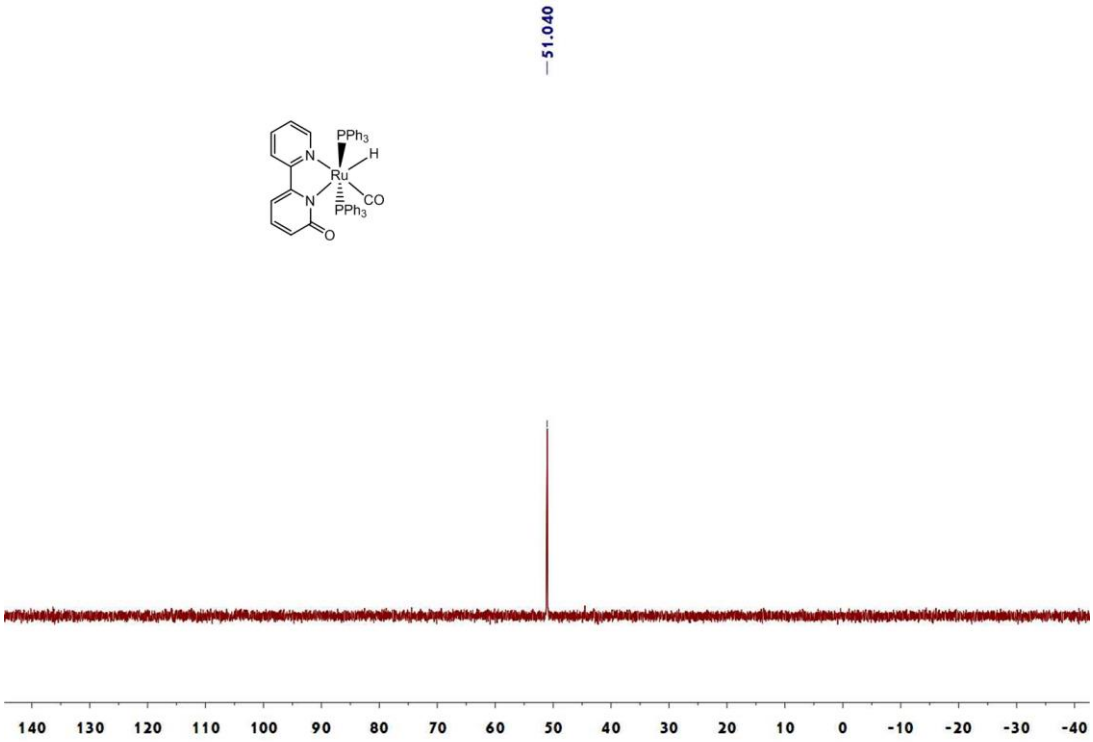


Fig. S33 $^{31}$P NMR spectrum of **5** in DMSO-$d_6$.

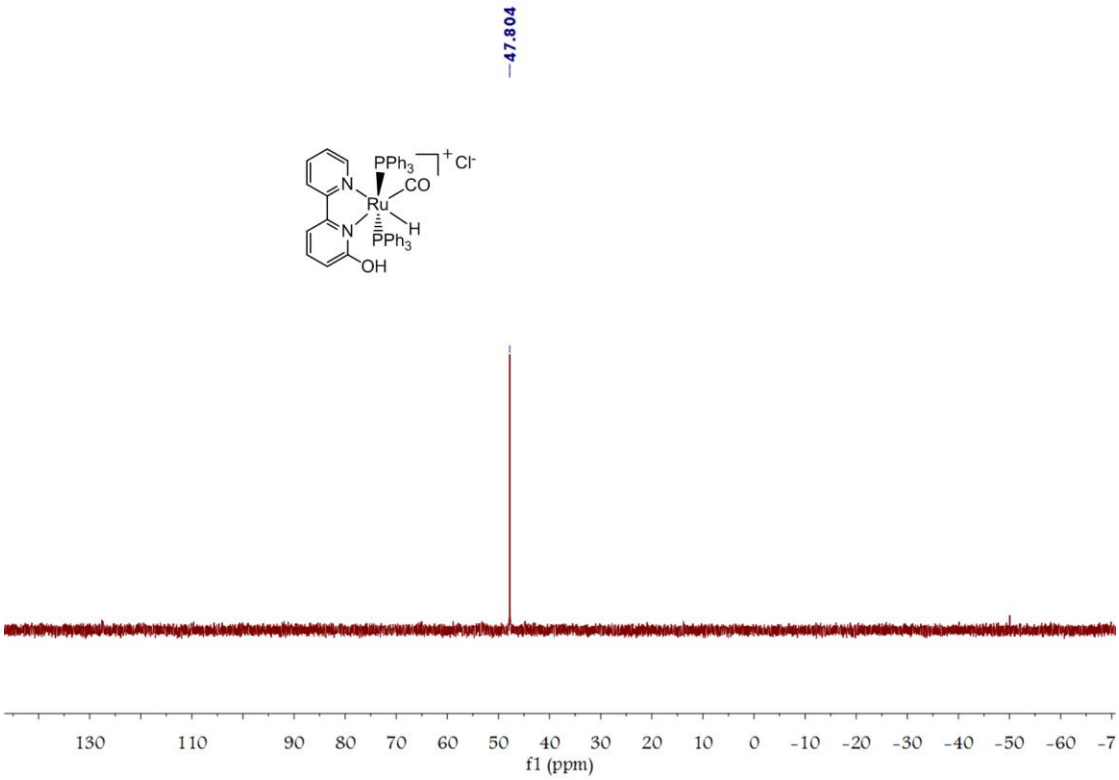


Fig. S34 $^{31}$P NMR spectrum of **6** in DMSO-$d_6$.

## $^{13}$C NMR Spectrum

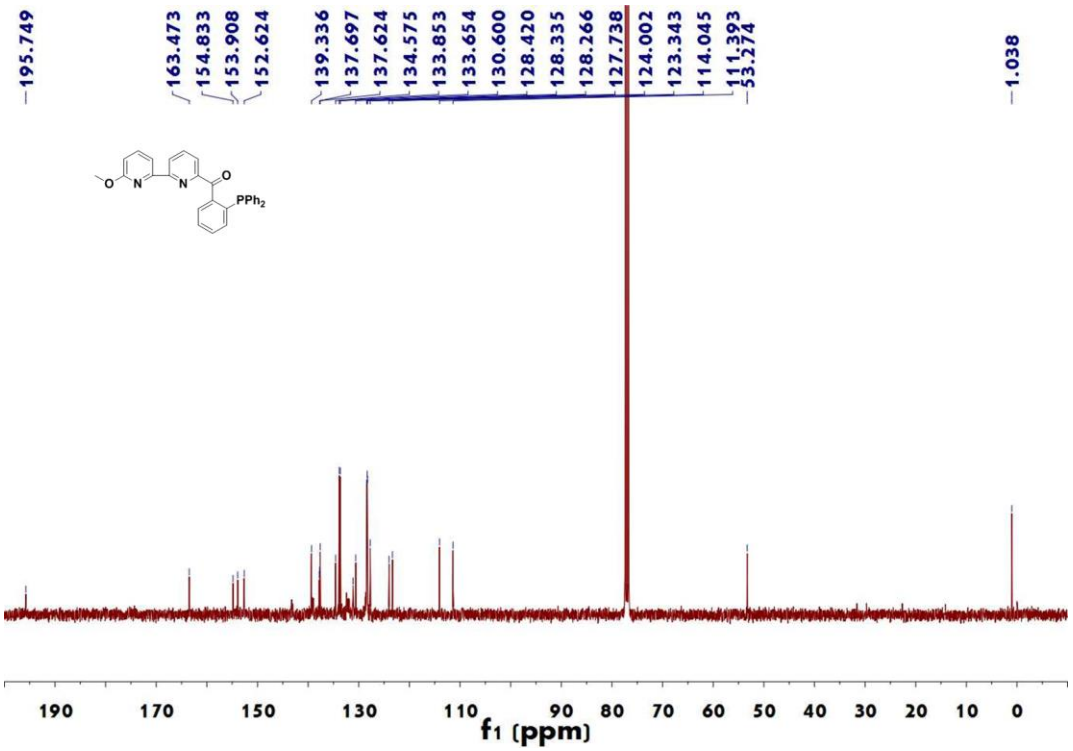


Fig. S35 $^{13}$C NMR spectrum of **L$_1$** in $CDCl_3$.

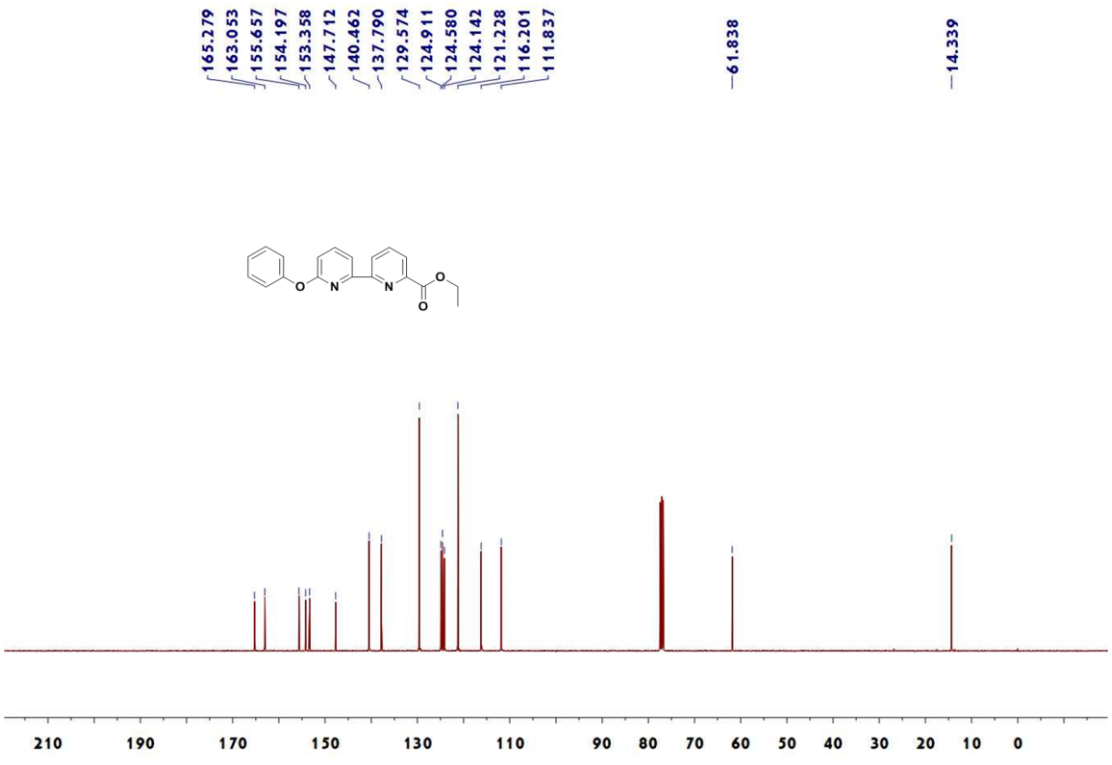


Fig. S36 $^{13}C$ NMR spectrum of ethyl 6-(6-phenyloxypyridin-2-yl)pyridine-2-carboxylate in $CDCl_3$.

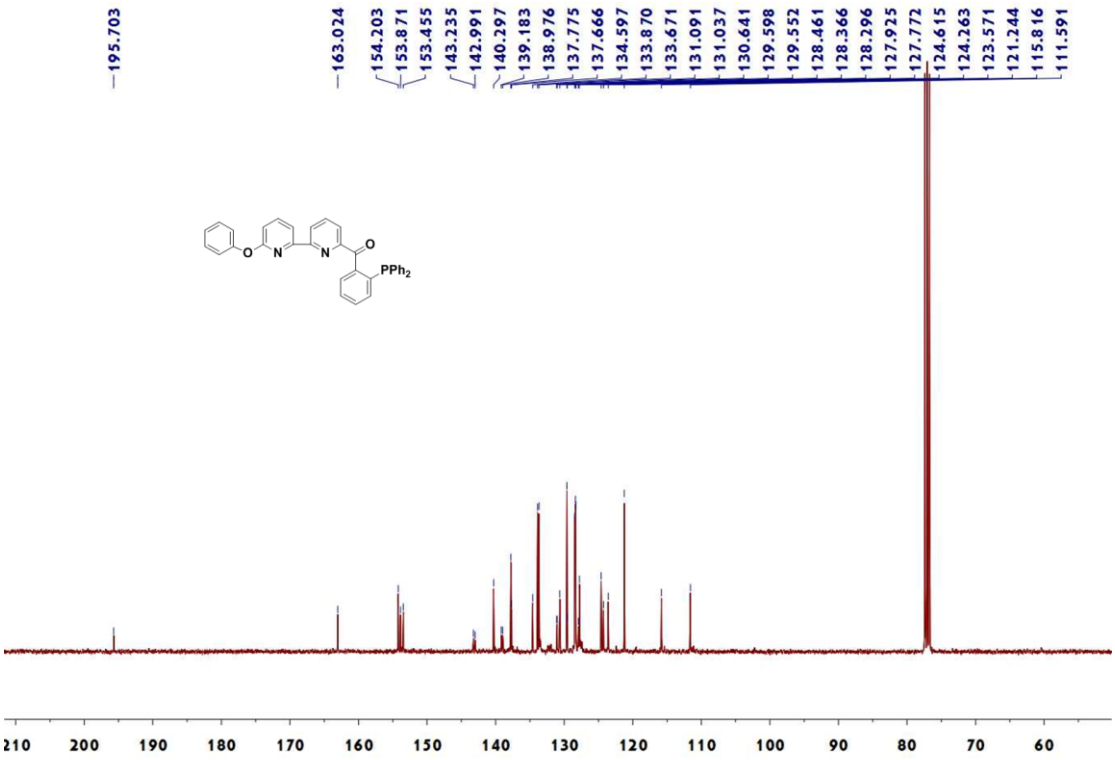


Fig. S37 $^{13}C$ NMR spectrum of **$L_2$** in $CDCl_3$.

# HR-MS Spectra

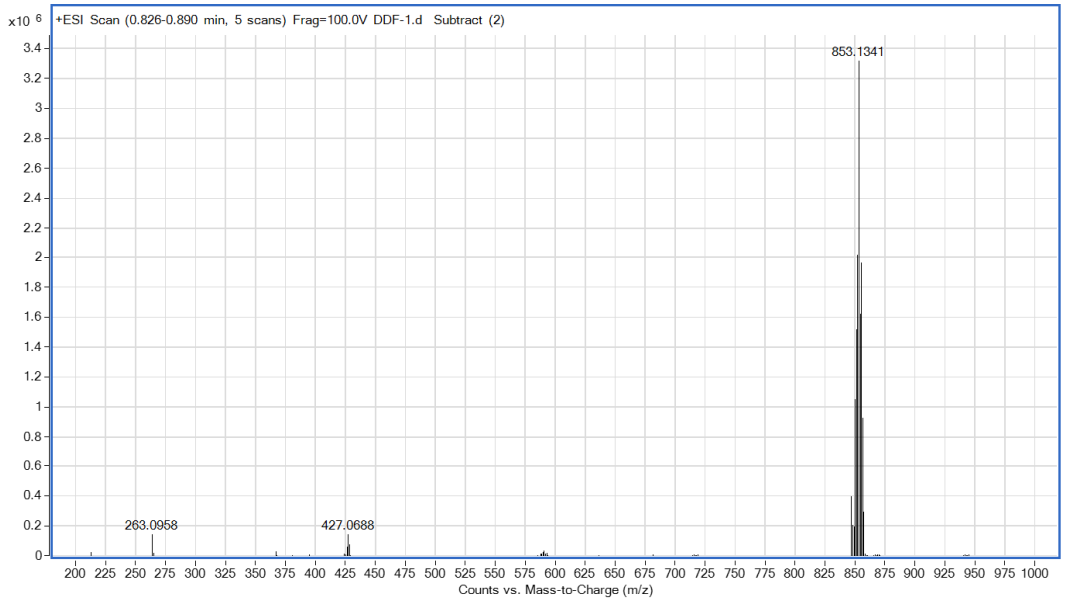


Fig. S38 HR-MS spectrum of complex **2**.

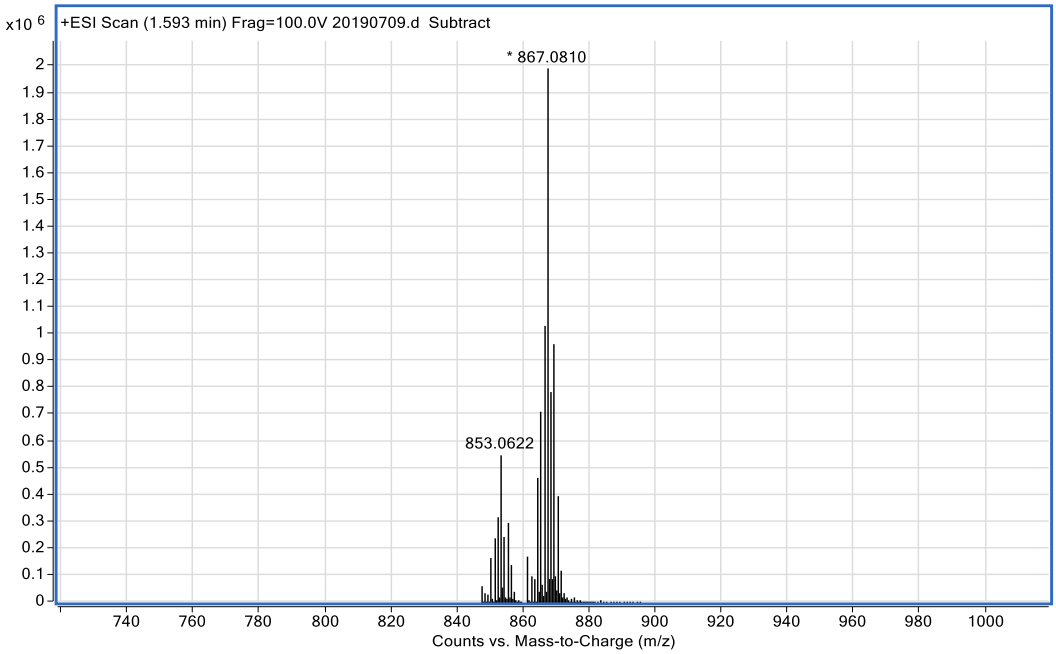


Fig. S39 Reaction of complex **1** with $H_2{}^{18}O$ (The peak at 853.0622 ($[M+H]^+$) belongs to **2**, and the peak at 867.0810 ($[M-Cl]^+$) belongs to the cation of **1**).

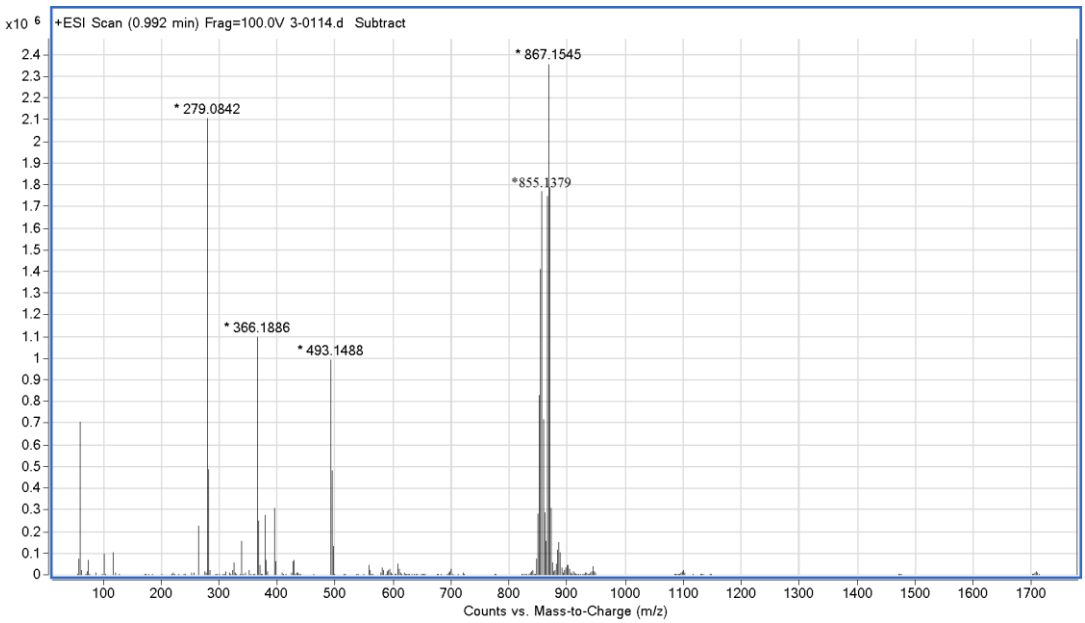


Fig. S40 Reaction of complex **1** with KOH/$H_2{}^{18}O$ (The peak at 855.1379 ($[M+H]^+$) belongs to the **$^{18}$O-substituted 2**, and the peak at 867.1545 ($[M-Cl]^+$) belongs to the cation of **1**).

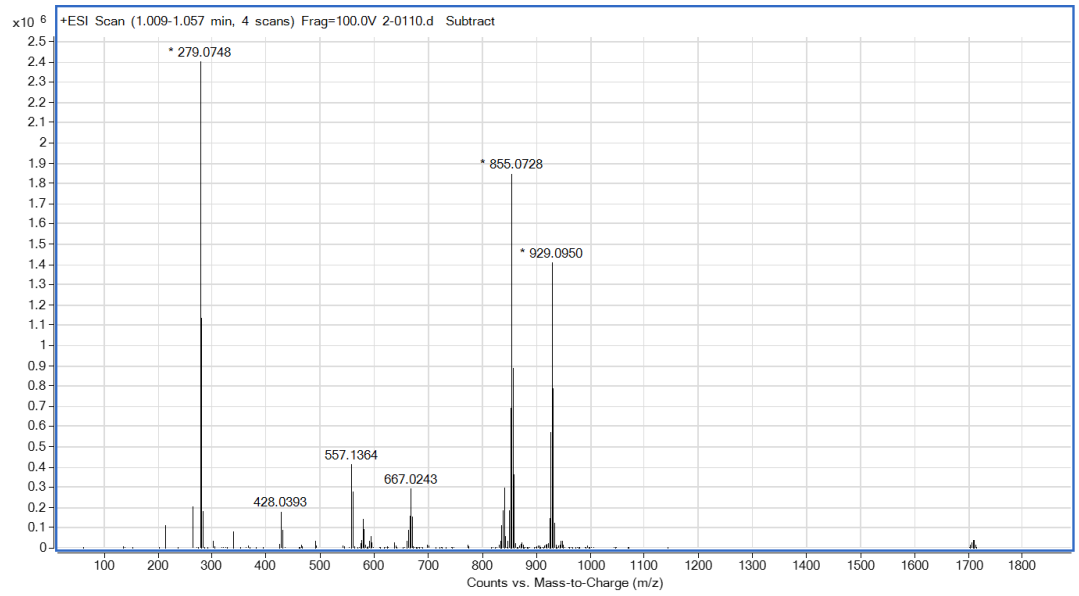


Fig. S41 Reaction of complex **3** with KOH/$H_2{}^{18}O$ (The peak at 855.0728 ($[M+H]^+$) belongs to the **$^{18}$O-substituted 2**, and the peak at 929.0950 ($[M-Cl]^+$) belongs to the cation of **3**).

# GC Analysis

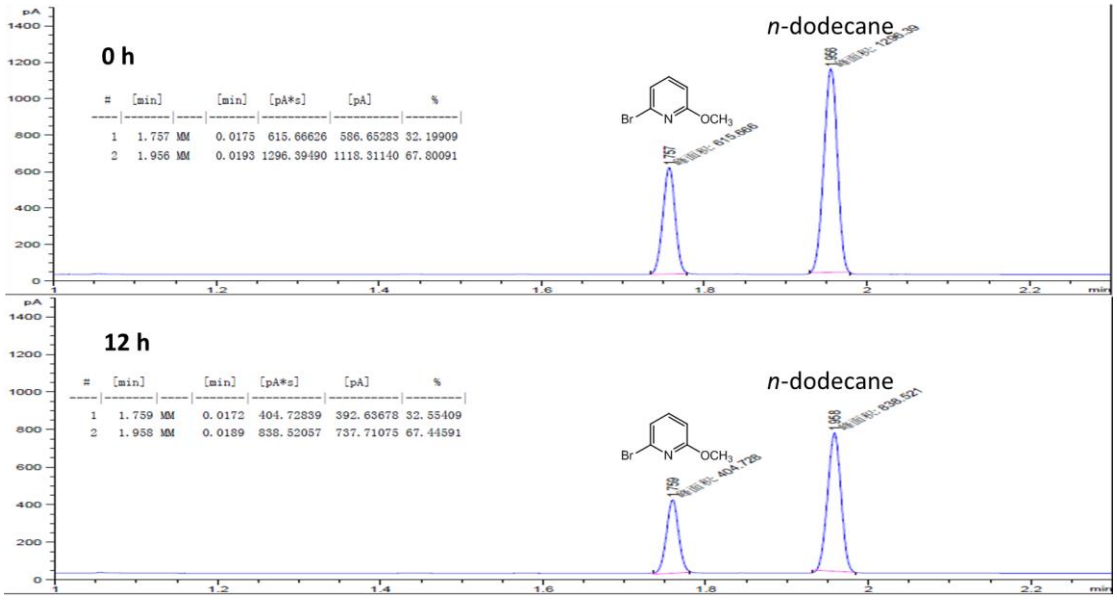


Fig. S42 GC analysis for Reaction of $RuHCl(PPh_3)_3(CO)$ with 2-bromo-6-methoxypyridine.

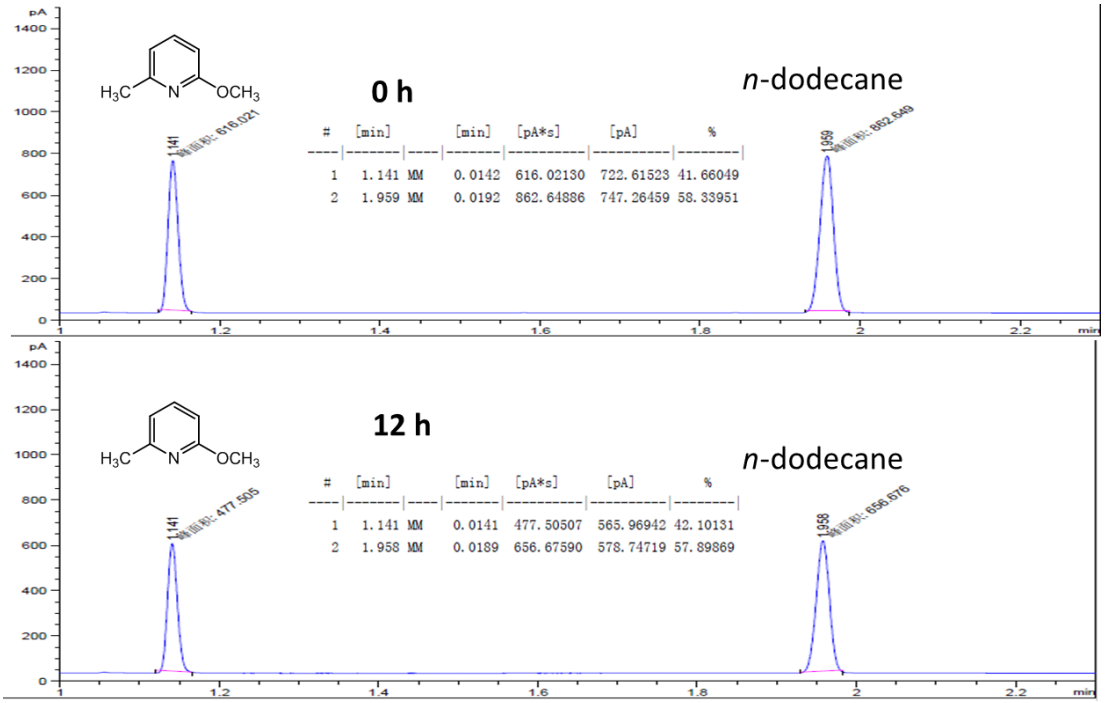


Fig. S43 GC analysis for Reaction of $RuHCl(PPh_3)_3(CO)$ with 2-methoxy-6-methylpyridine.